The importance of niches in defining phytoplankton functional beta diversity during a spring bloom

Arnaud Louchart, Fabrice Lizon, Elisabeth Debusschere, Jonas Mortelmans, Machteld Rijkeboer, Muriel Crouvoisier, Emeline Lebourg, Klaas Deneudt, François G Schmitt, Luis Felipe Artigas

Spatial niches of phytoplankton functional groups assessed during a spring bloom development in two temperate coastal seas

Arnaud Louchart[1,2], François G. Schmitt[1], Elisabeth Debusschere[3], Fabrice Lizon[1], Jonas Mortelmans[3], Machteld Rijkeboer[4], Muriel Crouvoisier[1], Emeline Lebourg[1], Klaas Deneudt[3], and Luis Felipe Artigas[1]

[1]Univ. Littoral Côte d'Opale, Univ. Lille, CNRS, UMR 8187, LOG, Laboratoire d'Océanologie et de Géosciences, F 62930, Wimereux, France
[2]Department of Integrative Marine Ecology, Stazione Zoologica Anton Dohrn, 1-80121, Napoli, Italy
[3]Flanders Marine Institut (VLIZ), Wandelaarkaai 7, 8400 Oostende, Belgium
[4]Laboratory for Hydrobiological Analysis, Rijkswaterstaat (RWS), Zuiderwagenplein 2, 8224 AD Lelystad, The Netherlands

Correspondence: Arnaud Louchart (arnaud.louchart@gmail.com) and Luis Felipe Artigas (felipe.artigas@univ-littoral.fr)

Abstract. We applied a pulse shape–recording flow cytometer (PSFCM) to address the whole phytoplankton community during the development of *Phaeocystis globosa* and diatom blooms, from the eastern English Channel (EEC) towards the southern North Sea (SNS), from late–April 2017 to mid–May 2017. The PSFCM recorded the optical properties at the single cell level allowing the characterization of phytoplankton as functional groups (PFGs). Both abundance and the calculation of the Local Contribution to Beta Diversity (LCBD) permitted to address the spatial segregation of PFGs from the most abundant to the marginal PFGs. The spatial segregation was studied through niche analysis and niche's overlap (NO). Coccolithophores were restricted to the Northern offshore waters of the the North Sea but they were the most abundant group in this area. *Synechococcus* and some picoeukaryotes groups sharing the same niches (NO > 0.60) were widespread along the southern coast of England in the English Channel. On the contrary, *P. globosa* and *Pseudo-nitzschia* groups were likely to be observed together (NO > 0.45) in the brackish waters flowing intermittently and discontinuously (tide- and coastal current-driven) from the Bay of Seine towards the Wadden Islands. The three life-stages of *P. globosa* were widespread in the southern and eastern coasts of both eastern English Channel (EEC) and southern North Sea (SNS). On the contrary, *Pseudo-nitzschia* was most abundant in the WRM ROFI. Finally, the beta regression allowed the prediction of the changes in community composition (i.e. LCBD values) influenced by positively by temperature and the distance to the coast and negatively by salinity. The contribution of the PFGs to these changes (i.e. SCBD) were positively linked to their niche position whereas it was negatively related to their environmental tolerance.

1 Introduction

Species distribution is the core of biodiversity research analyzing species and environmental interactions at different spatial and temporal scales. Nevertheless, the scale of variability of the distribution of a species depends, in the first place, on the abundance, physiology, size and metabolism of organisms and then, of the characteristics of the ecosystem and the processes to study. In marine ecosystems, coastal and marginal seas represent a boundary between open ocean and continental ecosys-

tems, being economically important as they represent between 22 % and 43 % of the estimated value of ecosystems services on Earth (Costanza et al., 1998). Hydrological, geochemical, geological and biological processes of the coastal ecosystem are continuously influenced by natural (e.g. turbulence, tides, winds, rivers run-off) and direct/indirect anthropogenic pressures (e.g. eutrophication, topography modification, contribution to global change) which lead to changes in the structure and processes, according to the timing and spatial extent of these events. In highly hydrodynamic areas, such pressures can generate patches at meso- and sub-mesoscale and make it particularly challenging to assess and understand the temporal and spatial distribution of phytoplankton (e.g. Cullen et al., 2002; Lovejoy et al., 2001; Seuront et al., 1999).

In aquatic and terrestrial ecology, nine hypotheses are often used to describe the relation between distribution and species abundance (Gaston et al., 1997; Gaston and Blackburn, 2008). Four hypotheses are related to data acquisition and data analysis whereas five are related to the ecology of species. Among the ecological hypotheses, habitat use is known to affect species occupancy and abundance because each species has its own niche and consequently may influence spatiotemporal variability of phytoplankton diversity. Species abundance related to their environment is often explained by species niche parameters (i.e. niche position and niche breadth). This concept is defined as the environmental space that a species can occupy according to their metabolic requirements and their abiotic parameters. To this, Hutchinson added the n–dimension feature in the fundamental niche where each dimension is represented by a factor of the environment (Hutchinson, 1957). Consequently, spatiotemporal patterns in species diversity should be related to niche parameters. First, Heino (2005) stated that niche hypothesis predicts that species having a marginal niche are less widely distributed and locally less common than species capable of occurring in average habitat conditions defined by the average environmental parameters used in the study. Therefore, it is assumed that species having the broader niche (non-marginal niche) have a wider regional occupancy. Secondly, the spatiotemporal index for diversity estimation such as the Species Contribution to Beta Diversity (SCBD) is related to niche position because species occurring in marginal habitats should occur in environmentally more restricted conditions than non-marginal species.

The identification and quantification of phytoplankton species is mainly based on morphology and processed by microscopy which misses most cells below 10 µm (Rutten et al., 2005). Moreover, species occurring in the same community which have similar traits may reveal 'redundancy' in ecological functions (Salmaso et al., 2015). As a consequence, using trait–based analysis focusing on individual phenotypes rather than species appears to be more relevant in understanding ecosystem functioning by avoiding this redundancy (Fontana et al., 2014). Grouping species together based on similar morphological, physiological and ecological features such as traits, defines functional groups (Litchman and Klausmeier, 2008) and reflects a functional diversity within a community. Most of the traits used to characterize the functional groups are morphological and physiological traits and, if required, some taxonomical (Salmaso et al., 2015) and ecological information (e.g. silicifiers/calcifiers) can be added. Recently, studies showed this morphophysiological classification can be obtained using the optical features of the particles (single-cell and colonies) assessed by the "pulse shape–recording" flow cytometer (Fontana et al., 2014; Fragoso et al., 2019).

In coastal areas, phytoplankton blooms often last from a week to one or two months. In coastal ecosystems particularly characterized by high hydrodynamics, current sampling strategies (discrete stations sampled weekly, fortnightly or monthly) can miss short-term events as well as the onset of blooms, local and/or sub-mesoscale patches and their spatial extension,

which can lead to misinterpretations of their importance for trophic networks and biogeochemical cycles and to insufficient measures to deal with harmful events. The eastern English Channel (EEC) and the southern Bight of the North Sea (SNS) are tightly connected areas of the two marginal seas (English Channel and North Sea) under the influence of Atlantic waters flowing from the Celtic Seas, the Atlantic eastern Shelf waters and from the North of the North Sea. Several rivers contribute to bring freshwater and nutrients into these areas mainly the Seine, the Somme, the Thames and the Westerschelde-Rhine-Meuse estuaries, which inputs form Regions of Freshwater Influence (ROFI). The spread of riverine inflow depends on river flow, tidal and coastal currents, as well as on main winds resulting in French eastern English Channel coasts to a brackish "coastal flow" (Brylinski et al., 1991). The bottleneck of the Dover Strait, contributes to drift waters towards the North (both brackish coastal waters and offshore Atlantic waters). In spring, phytoplankton biomass increases, benefiting of the winter nutrients stocks and the increase of light intensity. Spring blooms in these systems are characterized by the Haptophyte *Phaeocystis globosa* representing up to 80 % of the total biomass (Breton et al., 2000; Seuront et al., 2006), mainly along French, Belgian and Dutch coasts and is preceded, coupled to (Sazhin et al., 2007) and followed by diatoms blooms (Grattepanche et al., 2011; Schapira et al., 2008). Notwithstanding phytoplankton blooms are highly documented and benefit of long-term regular monitoring at discrete stations sampled weekly to fortnightly, the high hydrodynamical changing conditions experienced by these areas define different scales of variability that might be missed by reference monitoring approaches (Bonato et al., 2015, 2016; Louchart et al., 2020) and thus, generate an alternance of patches of high and low abundance (Louchart et al., 2020).

Recently, regular fortnightly monitoring on a discrete station in the EEC and SNS allowed a temporal study of the realized niche of *Phaeocystis globosa* (Karasiewicz et al., 2018). Nevertheless, in this highly hydrodynamical changing area (strong tidal forcing, tidal and haline fronts, ROFIs (e.g. Brunet and Lizon, 2003; Brylinski et al., 1996; Lacroix et al., 2004; Quisthoudt, 1987; Ruddick and Lacroix, 2006), studying the niches on discrete monitoring points can be inadequate to capture the natural variability. Increasing the frequency of monitoring is necessary to have a more reliable view of the system across spatial and temporal scales (Derot et al., 2015). For this purpose, innovative automated techniques were previously used to resolve spatial distribution of phytoplankton communities at high temporal and spatial resolution during the spring blooms either in the EEC or in the SNS (Bonato et al., 2015, 2016; Houliez et al., 2012; Thyssen et al., 2015).

Here, we aimed at following the spatio-temporal variations of phytoplankton spring blooms of diatoms and *Phaeocystis globosa* at the sub-mesoscale (< 10 km), from the eastern English Channel towards the Wadden Islands in the southern North Sea, and drifted northwards by both tidal and wind-induced currents. For this, we deployed an automated pulse shape–recording flow cytometry during on month (21 April 2017 to 18 May 2017) over three international and collaborative cruises (PHYCO–cruise, VLIZ–cruise and RWS–cruise). We addressed the spatial environmental niches of phytoplankton functional groups, covering the whole size–range of phytoplankton cells and colonies, following the spring bloom development in highly hydrodynamic areas under anthropogenic inputs. Our goals were: 1) to characterize phytoplankton functional groups distribution at fine spatial and temporal resolution during the spring bloom development from the eastern English Channel to the southern North Sea, 2) to determine which are the groups that mostly influenced the composition of the different communities characterized and by their relative changes in terms of abundance between areas, 3) to define how phytoplankton functional groups are arranged between them using their niche characteristics.

2 Materials and methods

2.1 Cruises outlines

Samples were collected during three international collaborative cruises in 2017 (Fig. 1) supported by French, Dutch and Belgian national and/or local projects (i.e. CPER MARCO for France and Monitoring Waterstaatkundige Toestand des Lands for RWS), in the frame of the Joint European Research Infrastructure for Coastal Observatories – New EXpertise (JERICO–NEXT) and LifeWatch European projects (H2020). The cruises started in well-established bloom conditions in the eastern English Channel before their spread in the southern North Sea waters. From April 21 to 30, 2017, the PHYCO cruise onboard the RV *Côtes de la Manche* (CNRS–INSU, Artigas, 2017) focused on a round trip within the eastern English Channel (from the Seine River and Portsmouth to the strait of Dover). Then, round-trips were carried out from French (EEC) and Belgian coastal waters (SNS) and the Scheldt-Rhine-Meuse plume to English coastal waters by the strait of Dover and the Thames dilution plume during the VLIZ cruise (8 to 12 May 2017) onboard the RV *Simon Stevin* (VLIZ). During the MWTL RWS cruise onboard the RV *Zirfaea* (15 to 18 May 2017), a round-trip started from the Rhine, Meuse and Scheldt and went towards the Wadden Islands and almost to the German Bight. In the three cruises, seawater was pumped continuously at 3 m depth through a circulation device and analyzed with an automated pulse shape–recording Flow Cytometer (PSFCM) to track and record phytoplankton cells and colonies every 10 min. In addition, continuous parameters were obtained by the thermosalinometer (PHYCO cruise) and FerryBoxes (VLIZ and RWS cruises).

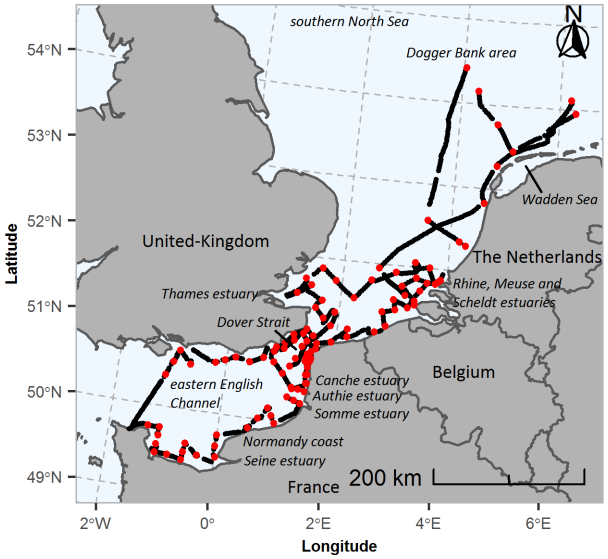

Figure 1. Studied area of PHYCO (CNRS–LOG), JERICO–NEXT/LifeWatch (VLIZ) and MWTL (RWS) cruises in the eastern English Channel (PHYCO and JN/LW cruises), southern North Sea and along the Wadden Islands (JN/LW and MWTL cruises) from April 21 to May 17, 2017. Black dots represent the continuous measurements recorded with the thermosalinometer and the CytoSense© flow cytometer. Red dots represent the discrete sampling stations investigated during the three cruises.

2.2 Discrete measurements

Samples for nutrient analyses were collected at 104 discrete stations (Fig. 1, PHYCO cruise: 47, JERICO–NEXT/LifeWatch cruise: 43 and MWTL cruise: 14). For PHYCO cruise, samples were collected and directly frozen. For JERICO–NEXT/LifeWatch and MWTL cruises, samples were filtered onto Whatman GF/F filters and kept frozen at -18 °C until analyses. Analyses of ammonium ($NH4^+$), nitrite (NO_2^-), nitrate (NO_3^-), phosphate (PO_4) and silicates (SiO_3) were processed by each institute for the respective cruise (CNRS–LOG for PHYCO cruise, VLIZ for JERICO–NEXT/LifeWatch cruise, RWS for MWTL cruise). Nutrients were analyzed according to Aminot and Kérouel (2004) in an Alliance auto-analyzer for CNRS-LOG. Detailed procedure for the RWS can be found in (Aardema et al., 2019) and for VLIZ in (Mortelmans et al., 2019). In the present study, only ratios between nutrients will be presented as nutrients were analyzed on three different sensors but using the same protocols.

2.3 Underway measurements

2.3.1 Hydrological parameters

The high resolution environmental data set included temperature, salinity, bathymetry and distance to the coast. Temperature and salinity were recorded every 15 s by a thermosalinometer (PHYCO cruise) or Ferryboxes (JERICO–NEXT/LifeWatch

and MWTL cruises). The data were averaged every 10 min to match phytoplankton data set. Bathymetry was extracted from the General Bathymetry Chart of the Ocean (GEBCO). An R script was written to extract the distance from the coast of each record. Sampling was processed from 20 m to 136 km of the coast.

2.3.2 Automated flow cytometry

A second data set included phytoplankton abundance per phytoplankton functional group defined by flow cytometry analysis, using a CytoSub© and/or a CytoSense© (Cytobuoy b.v., the Netherlands) which are pulse shape–recording flow cytometers (PSFCM). The PSFCM is a powerful technique to analyze, count and characterize single-cells and colonies, in vivo and at high frequency, from 1 to 800 µm width and up to a few millimeters length. The PSFCM records a "pulse shape" (Dubelaar et al., 1999) derived from optical features of each single particle, after passing through a solid–state Sapphir laser (Coherent Inc, 488 nm, 50 mV), providing morphological and optical traits that reflect actual physiological traits (Fontana et al., 2018; Fragoso et al., 2019; Pomati and Nizzetto, 2013). The size of particles is addressed and derived from the forward scatter (FWS) after bead correction and is collected by a PIN photodiode. Internal (e.g. size of the vacuole) or external (e.g. presence of coccolithes) compositions are addressed by the sideward scatter (SWS). In addition, three types of fluorescence are recorded: red fluorescence (FLR; emission: 668–734 nm), orange fluorescence (FLO; emission: 604–668 nm) and yellow fluorescence (FLY; emission: 536–601 nm). Both fluorescence and SWS are recorded by a set of photomultipliers. We established a low trigger level on the red fluorescence (range between 10 to 14 mV) in order to separate phytoplankton from non-autofluorescent particles (Thyssen et al., 2015). Finally, the sensor was equipped with a camera, providing pictures of the largest cells > 20 µm allowing coarse taxonomical recognition (Dugenne et al., 2014; Pereira et al., 2018). The CytoClus©software (Cytobuoy b.v., the Netherlands) allowed the visualization and characterization of the groups by the combination of features (Length, Total, Maximum) of the five signals recorded (FWS, SWS, FLR, FLO, FLY) mapped in 2–dimensions dot plots (cytogrammes). The amplitude and the shape were used to discriminate groups between them. Particles sharing similar optical properties (i.e. features and signals) were gathered together using the CytoClus© software (CytoBuoy b.v.) by gating a bulk of similar particles. According to the definition given by Reynolds (1997), phytoplankton sharing similar morphological, physiological and/or ecological properties such as calcifiers (coccolithophores) or silicifiers (diatoms) can be grouped together to form what is called Phytoplankton Functional Groups (PFGs). In our case, the different phytoplankton cytometry–defined groups were labelled from their optical characteristics, according to the criteria of the common vocabulary available on SeaDataNet https://www.seadatanet.org. Optical characteristics were based on anatomical, morphological and physiological properties of each cell/colony which reflected some traits of phytoplankton groups. Therefore, we chose to label them as Phytoplankton Functional Groups (PFGs). The main distinction between the PFGs was mainly based on the size (derived from ForWard Scatter) and the level of the red fluorescence (chlorophyll *a* autofluorescence), orange fluorescence (phycoerythrin autofluorescence) and yellow fluorescence (degraded pigments). Moreover, SideWard Scatter (SWS) of the PFG, also to sometimes characterizing sub-groups. In the study area during the spring bloom, the quasi–exclusive species within the nanophytoplankton groups are represented by *P. globosa* (Brussaard et al., 1996). Therefore, we tested the relation between nanophytoplankton groups sorted by the PSFCM (excluding cryptophytes and coccolithophores) and *Phaeocystis globosa* counts by microscopy Louchart et al.

(2018). We processed also images on a targeted area in the microphytoplankton group for subgroup visual validation. The size of particles was calibrated by a set of beads of 3 and 10 µm, which helped us to define three phytoplankton groups according to the size: Picophytoplankton (< 1-3 µm), Nanophytoplankton (3-20 µm) and Microphytoplankton (> 20 µm). According to Bonato et al. (2015), the estimated size, obtained by the length FWS of the PSFCM, was corrected by a correction factor (Eq. 1) obtained by the ratio of real beads size over the measured beads size. Thus, we applied this correction factor to the measured particles size to have the estimated particle size (Eq. 2).

$$Correction\,factor = \frac{Real\,beads\,size}{Measured\,beads\,size} \tag{1}$$

$$Estimated\,particule\,size\,(\mu m) = Measured\,particle\,size \times Correction\,factor \tag{2}$$

2.4 Data analysis

2.4.1 Water types

Within the whole study area, we defined water types from high frequency data (temperature, salinity, bathymetry and distance to the shore) by a three step procedure: 1) computation of a Euclidean distance matrix on standardized data (temperature, salinity, distance to the shore and bathymetry). 2) Processing a hierarchical agglomerative classification by the Ward method. 3) Getting the optimal number of areas when the highest Calinski-Harabasz criterion value was obtained. This procedure has also been described in (Louchart et al., 2020).

2.4.2 Local and Species Contribution to β–Diversity

Our three cruises defined a set of phytoplankton functional groups combined into phytoplankton communities. First, we ran the Local Contribution to Beta Diversity in order to highlight the spatial changes in the community functional composition (Legendre and De Cáceres, 2013). Briefly, the LCBD is a comparison of the uniqueness of each site to beta diversity. This analysis considers the species richness and the abundance of each species per site. Therefore, it is particularly suitable for high frequency datasets even though we did not consider species but functional groups. Prior to the analysis, the data were transformed by the Hellinger transformation. This transformation is strongly recommended for abundance data and especially in the use of the LCBD (Legendre and De Cáceres, 2013). The cytometry-defined functional groups were found in almost each location except for *Pseudo-nitzschia* spp for which the absence was defined as null abundance. NanoSWS, an other marginal PFG, were also found everywhere but its abundance was especially very high near the Dogger Bank. Therefore, the variability in LCBD depended only on the relative abundance of each ecological unit (define here as a PFG) in each site and should highlight changes in community structure (Rombouts et al., 2019). The computation of the β–diversity provided also the Species Contribution to Beta Diversity (SCBD) which is the degree of variation of individual species (in this case, of a phytoplankton functional group) across the study area. Calculations of both LCBD and SCBD were carried out using the

beta.div function of the adespatial package in R. Community changes between the water types were detected by averaging values of the total LCBD for each water type. LCBD values amongst areas were tested by Mann-Whitney test and Tukey-HSD post-hoc. The calculation of the SCBD for each water type allow the identification of the PFGs which contributed the most to the changes in term of community composition.

2.4.3 Niche parameters

To determine the relation between PFGs and the environment at a fine resolution scale, we calculated the niche position and niche breadth using the Outlying Mean Index (OMI) by following the procedure described by Dolédec et al. (2000), adapted to PFGs. This is a multivariate index which allows the quantification of niche parameters and explaining the variability of species to a selected set of environmental factor (Dolédec et al., 2000; Karasiewicz et al., 2017). Here, niche parameters were established for high resolution phytoplankton dataset (i.e. abundance recorded by the automated flow cytometer) and calculated using the high resolution abiotic dataset (i.e. temperature, salinity, distance to the shore and bathymetry). The OMI provides us the marginality and its variance part called the tolerance per PFG. A PFG that showed low values of OMI had non-marginal niches and thus occurred in common habitats (i.e. everywhere). On the contrary, a PFG that showed high values of OMI had marginal niches and therefore, occurred in specific habitats. PFGs that showed low values of tolerance had a narrow niche breadth whereas, PFGs that showed high values of tolerance had a wide niche breadth. The statistical procedure is detailed in Dolédec et al. (2000). The OMI analysis was conducted using the niche function of the ADE4 package, establishing the significance value of the relevant indexes at $p < 0.05$, based on 1000 random permutations data.

The usual procedure to characterize niche position and niche breadth per subset (subniche) until recently was to process several OMI analyses, one per subset. Nevertheless, this method assumed a unique origin of each subset of environmental conditions. In the case of different environmental conditions, the niches' positions vary between the subsets, thus the use of several OMI cannot rely accurately a comparison of the subsets. For this purpose, the WitOMI analysis developed by Karasiewicz et al. (2017) defined a common origin for the overall analysis and an origin for each subset. The calculation of the WitOMI was carried out by the subniche function of the R package subniche (Karasiewicz et al., 2017). Both marginality and tolerance were obtained for the OMI and WitOMI analysis. The marginality is defined as the distance between the mean habitat conditions used by the functional unit and the mean habitat conditions over the entire studied area. The tolerance corresponds to the niche breadth which refer to the variability of the environment used by the functional units. In addition, the residual tolerance is calculated and represents the part of the variance which is not explained by the environment.

The last procedure of the niche analysis at fine scales assesses how the groups are arranged between them. For this purpose, we estimated the niche overlap based on the method of Broennimann et al. (2012). This procedure uses a kernel density estimation (kde function of the ks package for R) weighted by the abundance of each group to create an occurrence density for each phytoplankton group. The coordinates of the kernel were set by the first two axes of the OMI analysis (following the procedure of Hernández-Fariñas et al. (2015)). We set our space grid ($r \times r$) for the kernel with $r = 100$. The comparison between two phytoplankton groups were then assessed by the Schoener D metric which quantifies the percentage of commonness between groups (Schoener, 1970). The overlap statistic (Eq. 3) is given by:

$$D_{1,2} = 1 - \frac{1}{2}\left(\sum_{ij} |p_{1ij} - p_{2ij}|\right) \quad (3)$$

Where p_{1ij} is the relative abundance of group 1 at the site *ij* and p_{2ij} is the relative abundance of the group 2 at the site *ij*. Additionnally to fine scales niches analysis, a 1–dimension kernel density estimation (KDE) was also processed for each nutrient ratios and each phytoplankton group based on the discrete sampling. This analysis provides the observed distribution of each PFG for continuous data. In our case, the KDE provides the affinity of each phytoplankton group for each nutrient during this snapshot of the year 2017.

2.4.4 Deterministic model

Finally, we used the beta regression to model the β–diversity indices responses (LCBD and SCBD) with the environmental parameters and the niche features. This method is particularly suitable to model the distribution of response variables within the interval [0;1] such as the LCBD and SCBD. We processed the beta regression and the logit link function in two separate models. First, the LCBD was modelled with 4 environmental parameters as predictors (temperature, salinity, bathymetry and the distance to the shore). We used only these 4 environmental parameters as their high recording frequency match the spatial resolution of the LCBD. The second model used the niche parameters (niche position and niche breadth) as predictors of the SCBD. The reduced model obtained produced a pseudo–R^2. The calculation of beta regression was processed on R using the betareg package.

3 Results

3.1 Hydrology

Temperature, salinity, bathymetry and distance to shore were variables recorded continuously. Silicates, nitrates, nitrites and phosphate were obtained at discrete stations. Continuous environmental parameters were used to define water types and then plotted on a TS diagram (Appendix A1) at fine scales whereas nutrients were used to supplement niche analyses. The temperature was 11.36 ± 0.68 °C. The minimum of temperature reached 9.83 °C the 15 of May near the northern point sampled during the survey whereas the maximum was 15.24 °C reached the 18 of May near the southern Dutch coast. Salinity was 34.01 ± 0.80. Minimum salinity was 29.33 and recorded near the coast and southern to the Meuse estuary the 18 of May. Maximum salinity reached 35.30 and was recorded on the way to transect to the farthest sampling station of the North Sea.

Ninety-fifth percentile for the nutrients (µM) ranged from for [0.03;19.94] for ammonium, [0.03;49.94] for Nitrates, [0.02;1.96] for Nitrites, [0.31;69.04] for Silicates, and [0.02;6.02] for Phosphate. Therefore, ninety-fifth percentile were [3.41;113.30] for N:P ratio, [1.11;115.41] for Si:P and [0.04;3.47] for Si:N. Maps of log10 of nutrients ratios can be found in the suplementary material (Appendix A2). In the present study, salinity was negatively correlated to nutrients concentrations (ρNO_3^- = -0.58; ρNO_2^- = -0.38; ρNH_4^+ = -0.37; ρSiO_3 = -0.37; all significant at $p < 0.001$). On the opposite, temperature was

positively correlated to nutrients concentrations ($\rho NO_3^- = 0.38$; $\rho NO_2^- = 0.49$; $\rho PO_4 = 0.45$; $\rho NH_4^+ = 0.62$; $\rho SiO_3 = 0.42$; all significant at $p < 0.001$). Finally, the distance to the shore was positively and significantly related to nutrients ($\rho NO_2^- = 0.33$; $\rho SiO_3 = 0.29$; $\rho PO_4 = 0.47$; all significant at $p < 0.05$) which is coherent with the pre-bloom situation as nutrients close to the coasts are at high level because they have not been consumed yet by plankton.

3.2 Water Types

The amplitude of the four variables recorded at high frequency (temperature, salinity, distance to the shore and bathymetry, appendix Table A1) supported the fact that several water types were crossed during the three cruises (Aardema et al., 2019; Bonato et al., 2015). Indeed, eight water types were characterized. According to their location, water types were mapped on the Fig. 2. Characteristics of each water type have been reported in the supplementary material (appendix Table A1). Water type 1 was mainly observed along offshore waters of EEC English and French coasts, and both England and Belgium part of the SNS with no direct freshwater inputs, but also in some offshore sites of the Scheldt-Rhine-Meuse ROFI and the Wadden Islands. Water type 2 was defined along the English coast of the EEC and SNS as transiant waters between the offshore waters (WT1) and the vicinity of the coast. WT2 was also observed in the Thames ROFI. Water type 4 was represented by some French (Bay of Seine, Normandy and southern to the Bay of Somme), Belgian (Belgian Coastal Zone, southern to the Scheldt mouth) and Dutch coastal areas under water exchanges between the North Sea and the Wadden Sea. Water types 3 and 7 represented, respectively, the offshore waters of the EEC nearby the western English Channel and in the Dover Strait (WT3) and the offshore waters of the North Sea at the vicinity of the Dogger Bank (WT7). Water type 5 corresponded to the offshore waters of the SNS. Finally, water types 6 and 8 represented waters by the Scheldt-Rhine-Meuse estuaries and near the southern Wadden Islands. The water type 8 being the most brackish water type (mean temperature was higher and mean salinity was lower than any other WTs; supp. material table 1).

3.3 High frequency flow cytometry

Up to 11 phytoplankton functional groups (PFG) were characterized during the 3 cruises. According to the correction size's formula provided by Bonato et al. (2015) and the common vocabulary in SeaDataNet, we could characterized 4 picophytoplankton, 5 nanophytoplankton and 2 groups larger than 20 µm (*Pseudo-nitzschia* and the rest of Microphytoplankton) with a size range from 1.99 ± 0.45 µm for *Synechococcus* to 33.45 ± 10.25 µm for Microphytoplankton (appendix Table A2). A strong spatiotemporal heterogeneity in phytoplankton distribution was evidenced (Fig. 3). The overall most abundant groups exhibited up to 10^5 cell cm^{-3} including PicoLowFLR (max: 1.51 10^5 cells cm^{-3}) and NanoHighFLR (max: 1.29 10^5 cells cm^{-3}). The less abundant groups never exceeded 1.00 to 3.00 10^3 cells cm^{-3}, they were Cryptophytes (max: 2.72 10^3 cells cm^{-3}) and Microphytoplankton (max: 9.40 10^2 cells cm^{-3}). Some PFGs sometimes exceed 10^4 cell cm^{-3}: *Synechococcus* (max: 1.47 10^4 cells cm^{-3}), PicoVeryLowFLR (max: 9.72 10^4 cells cm^{-3}), PicoHighFLR (max: 2.03 10^4 cells cm^{-3}) and Coccolithophores (max: 2.03 10^4 cells cm^{-3}). NanoFLR PFGs (NanoLowFLR, NanoHighFLR and NanoVeryHighFLR) were the dominant PFGs in the Strait of Dover and in French EEC waters under direct influence of Somme, Authie and Canche estuaries ("coastal flow"), in the Thames plumes as well as along the Belgian coast, in the Rhine, Meuse and Scheldt (ROFI) and along the Wad-

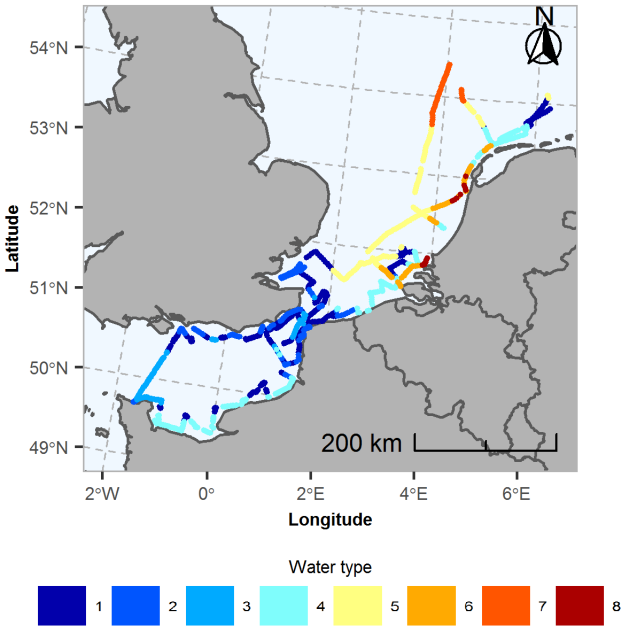

Figure 2. Water types discriminated from temperature, salinity, distance to the shore and bathymetry.

den Islands (SNS). They contributed to more than 50 % of the total abundance and often reached up to 2.00 10^4 cells cm^{-3}. A Spearman rank correlation on discrete stations of the PHYCO-CNRS and RWS-MWTL cruises gave a strong and significant correlation ($\rho = 0.75$, $p < 0.001$) between the NanoLowFLR, NanoHighFLR and NanoVeryHighFLR combined together and the microscopy counts of *Phaeocystis*. In this area, we also characterized a group composed of a pulse shape with symmetric and narrow cells and two symmetric chloroplasts. According to the images obtained by the camera mounted on the flow cytometer (see description in Pereira et al. (2018)), we could label the group as *Pseudo-nitzschia* spp. Nevertheless, low but significant Spearman rank correlation was found for this group between the PSFCM and the microscopic counts ($\rho = 0.39$, $p < 0.001$; Louchart et al. (2018)). *Synechococcus* and picoeukaryotes (PicoVeryLowFLR, PicoLowFLR and PicoHighFLR) were the most dominant PFGs along the English coasts (except the Thames ROFI), the Normandy and the Bay of Seine in the EEC and in offshore waters of the SNS, reaching up to 90 % of the total abundance (Fig. 3).

3.4 Local and Species Contribution to β–Diversity

The sites with high and statistically significant values of LCBD (Fig. 4) corresponded to spatial and/or temporal changes or turnover in the PFG assemblage's composition. During the whole sampling period, 6.5 % of the sites showed values of LCBD > 1.1953 10^{-3} displaying spatial and/or temporal heterogeneous breakdown of the LCBD index. Relatively high values were calculated for some locations of the Bay of Seine during the PHYCO cruise, in some locations of both French and Belgian SNS coasts during VLIZ cruise, by the Scheldt-Rhine-Meuse ROFI and in a spot of offshore waters of the North Sea during

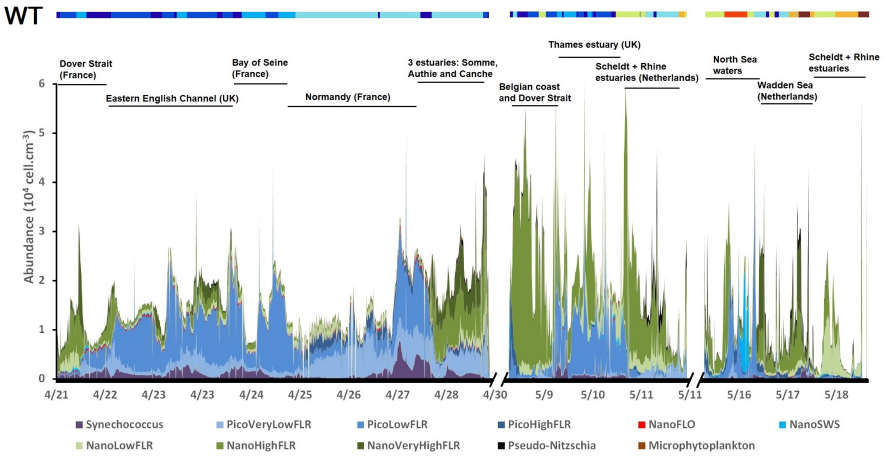

Figure 3. Spatial-temporal distribution of the phytoplankton groups sorted by the automated pulse shape–recording flow cytometer during the PHYCO cruise (04/21 to 04/30), the VLIZ cruise (05/08 to 05/11) and the RWS cruise (05/15 to 05/18).

the RWS cruise (Fig. 3). The sites of the Bay of Seine exhibited intermediate and significant values of LCBD which were attributed to the large dominance of the PicoLowFLR group. In the Belgian Coastal Zone (BCZ), during the VLIZ cruise, the significant high values of LCBD were attributed to the increase in *Pseudo-nitzschia* abundance. In the Westerschelde, Rhine and Meuse ROFI, the high significant LCBD values were explained by the increase in the NanoLowFLR contribution to the total abundance. Finally, central North Sea waters (at the Northern limit of the SNS) exhibited also high values of LCBD and corresponded to a large contribution of the Coccolithophores group (NanoSWS) to the total abundance (Fig. 4). Five PFGs have a SCBD above 10 %: PicoLowFLR (25 %), NanoHighFLR (17 %), PicoVeryLowFLR (17 %), NanoVeryHighFLR (13 %) and NanoLowFLR (10 %). They followed a spatial segregation between English coasts and the Rhine-Scheldt-Meuse-Seine ROFIs, the French EEC “Coastal flow” and along the Wadden Islands. The latter waters were dominated by NanoLowFLR, NanoHighFLR and NanoVeryHighFLR, separated by a few “buffer” areas with low values of LCBD formed by Normandy, French North Sea coast and Belgian Coastal Zone. None of the PFGs were dominant in these "buffer" areas.

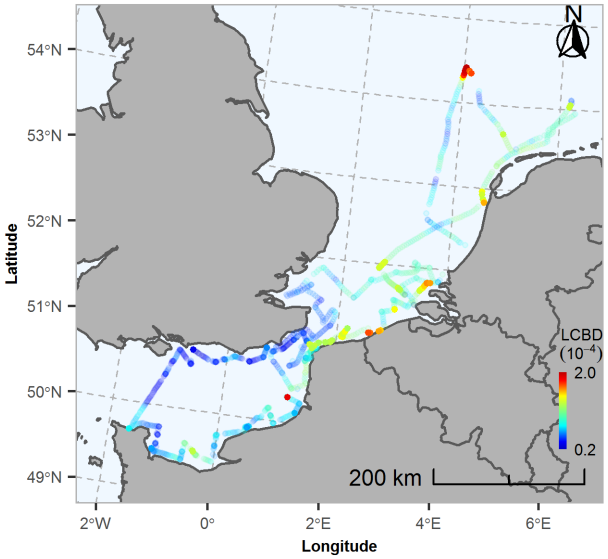

Figure 4. Map of the LCBD index values calculated on the abundance phytoplankton functional groups defined by PSFCM. Transparent dots correspond to non-significant LCBD values. Filled dots correspond to significant LCBD values.

3.5 LCBD and SCBD per Water Type

LCBD values made possible to address the extent of community changes across water types. A Mann Whitney test and Tuckey-HSD post hoc detected significant differences ($p < 0.05$) in the community composition through the LCBD values between the different water types (Fig. 5). The lowest values of LCBD were found between water types 1, 2 and 3 which, in turn, were slightly lower than the water type 4 (Fig. 5). In the southern North Sea, the values of LCBD were significantly different between water types 5, 6 and 8. LCBD of water type 7 was not significantly different from water type 5 and water type 8 but lower than water type 6 which showed the highest LCBD values of all.

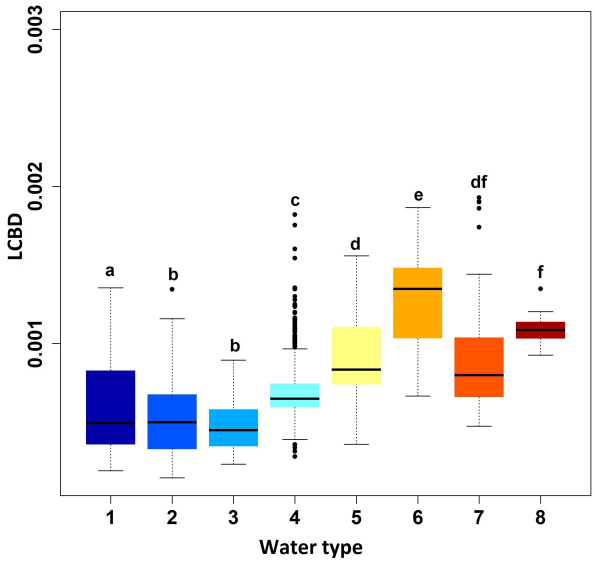

Figure 5. Boxplot of the LCBD values in each water type and their relations after Mann-Whitney and Tukey-HSD post hoc tests.

315 The calculation of the SCBD amongst water types gave the contribution of each PFG to the β–diversity for each water type. PFGs contributed unequally to the SCBD (Fig. 6). *Synechococcus* showed the highest contribution to β–diversity in water type 8 and the lowest in water types 5 and 7. Cryptophytes and, to a lesser extent, PicoHighFLR, showed low contribution to the SCBD in most water types. NanoLowFLR contributed the most to SCBD in water types 5 and 6. NanoVeryHighFLR showed its highest contribution to β–diversity in water types 5, 6 and 8 whereas it was co-dominant with PicoVeryLowFLR, PicoLowFLR
320 and NanoHighFLR group in the water types 1, 2, 3 and 4. In water type 7, there was a high contribution to β–diversity for the Coccolithophores. Microphytoplankton only contributed up to 6.99 % to the β–diversity.

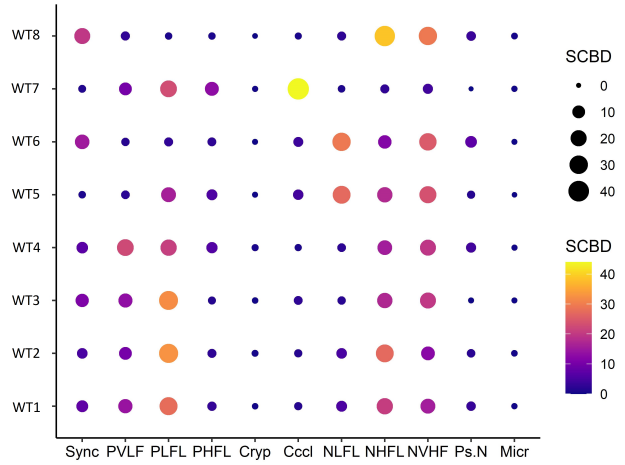

Figure 6. Species Contribution to Beta Diversity (SCBD) of each phytoplankton functional groups among the eight water types. SCBD is expressed in percent. The eleven PFGs are *Synechococcus* (Sync), PicoVeryLowFLR (PVLF), PicoLowFLR (PLFL), PicoHighFLR (PHFL), Cryptophytes (Cryp), Coccolithophores (Cccl), NanoLowFLR (NLFL), NanoHighFLR (NHFL), NanoVeryHighFLR (NVHF), *Pseudo-nitzschia* (Ps.N) and Microphytoplankton (Micr).

3.6 Niche analyses

The global test of the average marginality of the PFGs obtained by the OMI analysis was significant, thus indicating the influence of the environment on phytoplankton community structure (Monte Carlo test, $p < 0.001$). All the PFGs showed a
325 significant deviation of their niche from the origin (table 1). The 2 first axes of the OMI analysis represented 95 % of the total variance with 55 % of the total inertia explained by the first axis and 40 % by the second axis (Fig. 7). Axis 1 was explained by spatial gradients (offshore-inshore, East-West, North-South) whereas axis 2 was explained by environmental parameters.

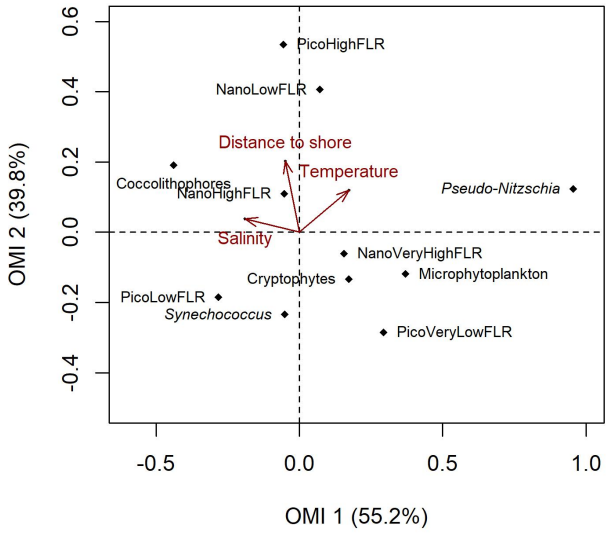

Figure 7. Outlying Mean Index (OMI) analysis of the eleven phytoplankton functional groups (PFG) characterized by the automated pulse shape-recording flow cytometry according to the four continuously-recorded environmental parameters. Bathymetry was removed from the plot as it was not significantly involved in the analysis

NanoHighFLR and NanoVeryHighFLR exhibited the lowest marginality (OMI: NanoHighFLR: 0.02, NanoVeryHighFLR: 0.03) with intermediate values of niche breadth (Tol: NanoHighFLR: 1.43, NanoVeryHighFLR: 1.83). Intermediate values of marginality were calculated for *Synechococcus* (OMI: 0.08), PicoVeryLowFLR (OMI: 0.17), PicoLowFLR (OMI: 0.11), Cryptophytes (OMI: 0.07), NanoLowFLR (OMI: 0.18) and Microphytoplankton (OMI: 0.16). Among these PFGs, *Synechococcus*, PicoLowFLR and Cryptophytes exhibited a wide niche breadth (Tol: *Synechococcus*: 0.43, PicoLowFLR: 0.87, Cryptophytes: 1.09). Despite microphytoplankton are probably the most diverse group of all PFGs in terms of species, they exhibited a very narrow niche breadth (Tol: 2.07). PicoVeryLowFLR and NanoLowFLR showed intermediate niche breadth (Tol: PicoVeryLowFLR: 1.35 and NanoLowFLR: 1.25). Finally, a high marginality was calculated for PicoHighFLR (OMI: 0.30), Coccolithophores (OMI: 0.28) and *Pseudo-nitzschia* (OMI: 0.92). PicoHighFLR and *Pseudo-nitzschia* exhibited intermediate niche breadth (Tol: PicoHighFLR: 2.01 and *Pseudo-nitzschia*: 2.44) whereas Coccolithophores exhibited the narrowest niche breadth (Tol: 3.33). *Pseudo-nitzschia* as well as Microphytoplankton were more likely observed, respectively, in warm and offshore waters (deeper stations), Coccolithophores were more abundant in the saltier waters and NanoLowFLR and PicoHighFLR have affinity for offshore waters. The other PFGs showed less restrictions regarding the environmental variables measured in the study area.

In addition to the ordination method, the Kernel Density Estimation plots (Fig. 8) revealed the 1-dimension responses of the eleven PFGs in relation to nutrient ratios (i.e. N:P, Si:N and Si:P) from discrete stations, over the whole study period (April 21 to May 18). From this, we found that six PFGs (*Synechococcus*, PicoVeryLowFLR, PicoLowFLR, NanoLowFLR, Cryptophytes and Microphytoplankton) showed a preference for high N:P ratio (peaks at N:P = 31). NanoHighFLR and NanoVeryHighFLR

Table 1. Niche parameters of the phytoplankton functional groups characterized in this survey.

PFG	Inertia	OMI	Tolerance	Residual tolerance (%)	p-value
Synechococcus	3.50	0.08	0.43	85.5	0.001
PicoVeryLowFLR	3.21	0.17	1.35	52.6	0.001
PicoLowFLR	3.53	0.11	0.87	72.0	0.001
PicoHighFLR	6.21	0.30	1.62	69.0	0.001
Cryptophytes	3.62	0.07	1.09	68.0	0.001
Coccolithophores	6.03	0.28	3.33	40.1	0.001
NanoLowFLR	4.81	0.18	1.25	70.3	0.001
NanoHighFLR	4.05	0.02	1.43	64.2	0.001
NanoVeryHighFLR	3.65	0.03	1.83	49.1	0.001
Pseudo-nitzschia	5.37	0.92	2.93	28.2	0.001
Microphytoplankton	4.00	0.16	2.07	44.3	0.001

high abundance was preferentially observed in areas with slightly lower N:P ratios (N:P = 16). Coccolithophores were abundant in water types characterized by low N:P ratio (maximal KDE for N:P = 2.5) whereas *Pseudo-nitzschia* were more likely observed in water types characterized by high N:P ratio (maximal KDE for N:P = 126). From the eleven PFGs considered in the present study, seven were very abundant (PicoHighFLR, NanoLowFLR, NanoHighFLR, NanoVeryHighFLR, Cryptophytes, *Pseudo-nitzschia* and Microphytoplankton) in water types characterized by Si:P ratio comprised between 10 and 100. The Si:P ratio of the water types where *Synechococcus*, PicoVeryLowFLR and PicoLowFLR occurred strongly, ranged between the limit of detection of the nutrients (Si and P) and 50. Consequently, their distribution would not be affected by the nutrients' concentrations of the study area, at this period of the year. The Coccolithophore group was more abundant in waters characterized by a ratio Si:P between 3 and 31 with a mean around the Redfield ratio (Si:P = 16). Concerning the Si:N ratio, all picophytoplankton groups (i.e. *Synechococcus*, PicoVeryLowFLR, PicoLowFLR and PicoHighFLR) were mainly observed in water types characterized by Si:N ratios below the Redfield ratio (i.e. Si:N = 1). However, the density of PicoVeryLowFLR showed a second mode, the second one being higher than the Redfield ratio. Cryptophytes were most abundant in water types characterized by low (< 1) Si:N ratios. NanoLowFLR, NanoHighFLR and NanoVeryHighFLR exhibited the same KDE plots. They were mainly abundant in water types where the Si:N ratio ranged between 0.1 and 10 but preferentially in water types with a Si:N ratio near the Redfield ratio. The Coccolithophores group was mainly observed in water types with a Si:N ratio above the Redfield ratio whereas the opposite pattern was observed for *Pseudo-nitzschia*. Finally, Microphytoplankton group was most abundant in water types with Si:N ratio below or equal to the Redfield Ratio and was widely distributed across the nutrient-ratio range.

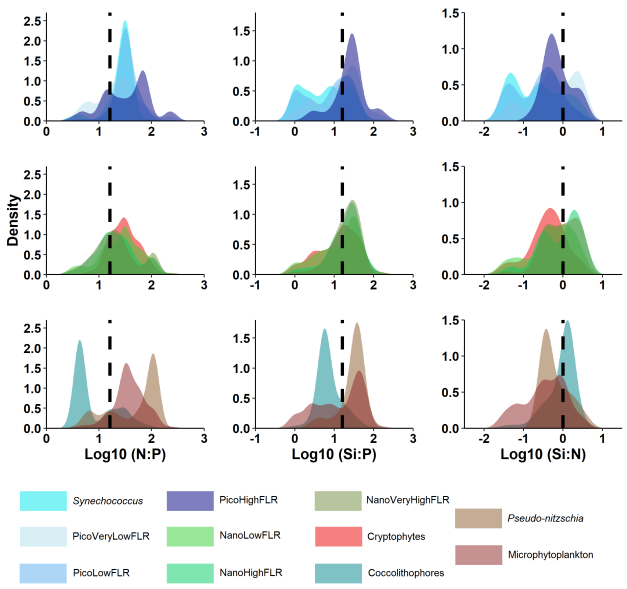

Figure 8. Kernel Density Estimation plots showing the frequency of abundance of each Phytoplankton Functional Group related to nutrient ratios. The dashed lines represent the logarithm of the Redfield ratios (i.e. N:P = 16; Si:P = 16; Si:N = 1).

3.7 Niche overlap

The Schoener Index is the similarity between the niche breadth (i.e. hypervolume of n dimensions where n is the number of variables used to define the niche breadth) of two organisms. Here, this index reveals the overlap between pairs of phytoplankton functional groups (Fig. 9). The niche overlap (NO) was comprised between 0.35 (*Pseudo-nitzschia* and PicoLowFLR) and 0.74 (*Synechococcus* and PicoLowFLR). We set arbitrary low NO for values below 0.45, intermediate NO for values of NO comprised between 0.45 and 0.60, high NO for values above 0.60. High NO was found between three picophytoplankton groups: *Synechococcus*, PicoVeryLowFLR and PicoLowFLR. The same trends were found between NanoLowFLR and NanoHighFLR and between NanoHighFLR and NanoVeryHighFLR. In addition, Coccolithophores exhibited high NO with *Synechococcus* and PicoLowFLR. Microphytoplankton showed high NO with all the phytoplankton groups except PicoHighFLR (low NO), NanoVeryHighFLR and *Pseudo-nitzschia* (intermediate NO). *Pseudo-nitzschia* had low NO together with picophytoplankton (*Synechococcus*, PicoVeryLowFLR, PicoLowFLR, PicoHighFLR), Cryptophytes and Coccolithophores. PicoHighFLR exhibited low NO with the three other picophytoplankton groups: *Synechococcus*, PicoVeryLowFLR and PicoLowFLR.

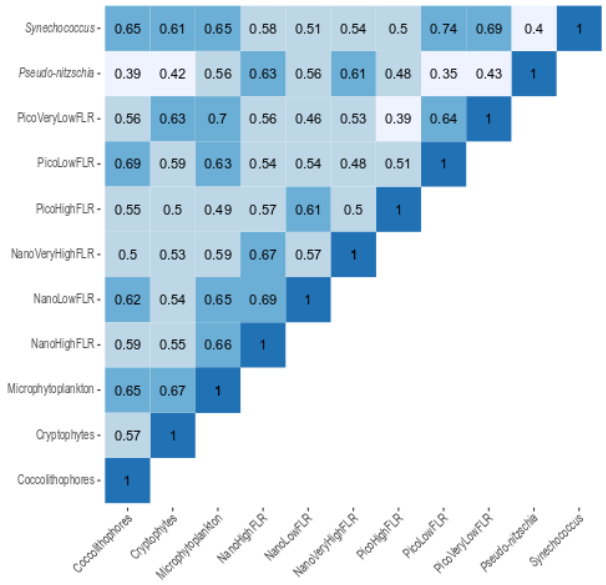

Figure 9. Upper correlation matrix representing pairwise overlap between the different phytoplankton functional groups defined by automated pulse shape-recording flow cytometry. Blue gradient, from light blue to dark blue, shows the increase in niche overlap. Below 0.45, the Schoener Index is low; from 0.45 to 0.59, values are intermediate and above 0.60, values of the Schoener Index are high

3.8 Deterministic model

Based on the high frequency data from the flow cytometer and the environmental variables considered, the beta-regression model of the abundance function of the environment, showed that environmental variables explained 37 % of the variation in the LCBD (table 2). Temperature and the distance to the shore explained positively and significantly ($p < 0.001$) the values of LCBD. Intercept and salinity were negatively and significantly ($p < 0.001$) related to the LCBD values. Bathymetry was not significant. As expected, niche position was negatively and significantly related to the SCBD in our second model. Contrariwise to expected results, niche breadth was negatively related to SCBE and the result was non-significant ($p > 0.05$). Consequently, the niche position of PFGs is a good estimator of the SCBD amongst the different water types. This latter model explained 13 % of the variance in the SCBD (table 2).

Table 2. Beta regression analysis of two responses variables: Local Contribution to Beta Diversity (LCBD) and Species Contribution to Beta Diversity (SCBD). The LCBD was explained by the continuous environmental data. The SCBD was explained by the PFG niche features (niche position and niche breadth. SE: Standard Error, df: degree of freedom, z: z-statistic (estimate divided by SE) and p: probability-value.

	Estimate	SE	df	z	p-value	Pseudo-R^2
(a) LCBD						
Intercept	-5.66	0.56	6	-10.15	0.001	
Temperature	0.22	0.01	6	15.02	0.001	
Salinity	-0.13	0.01	6	-9.39	0.001	
Distance to shore	0.01	0.004	6	19.44	0.001	
Bathymetry	-0.001	0.0009	6	-0.15	0.89	0.37
(b) SCBD						
Intercept	-2.06	0.21	4	-9.88	0.001	
Niche position	-2.92	1.10	4	-2.65	0.008	
Niche breadth	-0.16	0.40	4	-0.42	0.67	0.13

4 Discussion

4.1 High frequency flow cytometry

The present survey aimed at study the whole extent of the spring bloom through different systems more or less influenced by important estuarine inputs, from the Bay of Seine and the Thames to the Scheldt-Rhine-Meuse estuaries and along the Wadden Islands. This was only possible by an international cross-border combined approach within local, national (Dutch Monitoring Waterstaatkundige Toestand des Lands, Rijkswaterstaat and French CPER MARCO) and European projects (DYMAPHY, http://www.dymaphy.eu; LifeWatch project, http://www.lifewatch.be and JERICO-NEXT; https://www.jerico-ri.eu). Within these projects, recent integrative surveys have investigated spatial and temporal distribution of phytoplankton in part of our study area (Aardema et al., 2019; Bonato et al., 2015; Thyssen et al., 2015). In the EEC and SNS, phytoplankton blooms starts in late winter/early spring with a diatom bloom followed by or concomitant bloom of the Haptophyte *Phaeocystis globosa*, the latter alternating between a colonial stage (i.e. diploid free cells or colonial cells) in the mid phase and solitary cells (i.e. haploid free cells) at the initiation and the senescence of the bloom (Grattepanche et al., 2011; Guiselin, 2010; Lamy et al., 2009; Lefebvre et al., 2011; Peperzak, 1993; Rousseau et al., 2007; Seuront et al., 2006; Stelfox-Widdicombe et al., 2004). Such observations of these spatiotemporal successions of blooms were reported along the French, Belgian and Dutch coasts using microscopy (Breton et al., 2006; Gómez and Souissi, 2007; Grattepanche et al., 2011; Schoemann et al., 2005), HPLC-CHEMTAX method (Muylaert et al., 2006; Schlüter et al., 2000), multispectral fluorometry (Houliez et al., 2012), flow cytometry (Aardema et al., 2019; Bonato et al., 2015, 2016; Rutten et al., 2005; Thyssen et al., 2015) and molecular

approaches (Christaki et al., 2014; Genitsaris et al., 2015, 2016; Monchy et al., 2012; Rachik et al., 2018). Previous studies in the EEC and SNS reported the presence of three groups of *P. globosa* observed by automated flow cytometry (Bonato et al., 2015; Guiselin, 2010; Rutten et al., 2005). They are differentiated from each other by their amount of chlorophyll a (i.e. by the expression of the chlorophyll a autofluorescence-FLR) and their size. Following the correlation between the three NanoFLR groups, we labelled NanoLowFLR, NanoHighFLR and NanoVeryHighFLR as different life-stages of *P. globosa* (Guiselin, 2010; Peperzak, 1993; Rutten et al., 2005). NanoLowFLR and NanoHighFLR are stated to be haploid free cells of *P. globosa* and NanoVeryHighFLR is stated to be diploid free cells of *P. globosa* (Bonato et al., 2015, 2016). However, other autotroph nanoeukaryotes co-occurring with *P. globosa* are commonly evidenced in the Belgian and Dutch coast such as Chrysomonodales and Euglenophyceae (Prins et al., 2012). The low correlation between microscopy counts and cytometry abundance of *Pseudo-nitzschia* is a result of detecting a particle as a single-cell or a colony. The latter case can reveal a bias due to an under-estimation of the number of cells during colonial stage, considering that also *Pseudo-nitzschia* usually colonizes *Phaeocystis globosa* colonies at the last phase of the spring bloom (Sazhin et al., 2007).

In this survey, we also report a short-term spatiotemporal phenology of *P. globosa* bloom by characterizing its dominant life-stages among the spatial overlapped areas. The first spatial overlap occurred between PHYCO cruise (20 to 21 of April) and the VLIZ cruise (8 to 9 of May, VLIZ cruise). Over fifteen days between the two investigations of three French estuaries (Somme, Authie and Canche) and the Strait of Dover (continuum of brackish water influence called in the French EEC as "coastal flow", Brylinski et al., 1991), the abundance of the haploid and very fluorescent morphotype of *P. globosa* increased. Such observation might have represented the expansion phase of the bloom in which haploid highly fluorescent morphotype evolves to the diploid morphotype by sexual processes (Rousseau et al., 2007). In addition, at the end of the PHYCO cruise, the diploid life-stage of *P. globosa* (NanoVeryHighFLR) was very abundant in the French coastal waters of the "Coastal flow". This observation suggests the peak of the *P. globosa* bloom to occur in this area at the end of April. A second spatial overlap occurred also during the VLIZ and RWS cruises in the Scheldt-Rhine-Meuse ROFI. During the first recording time in this area (end of VLIZ cruise, 12 of May), the haploid and high fluorescent morphotype dominated the total NanoFLR abundance whereas six days later (end of RWS cruise, 18 of May), the second recording in the ROFI area was marked by a dominance of the haploid and low fluorescent morphotype. This latter observation in combination with the absence of the diploid morphotype relate the senescence of *P. globosa* bloom in the mid of May 2017 (Rousseau et al., 2007).

4.2 Local and Species Contribution to β–Diversity

4.2.1 Spatiotemporal dynamics

Spatiotemporal changes in the assemblage composition (in term of PFGs) was highlighted by calculating the LCBD which is a powerful analysis for high resolution datasets and which revealed changes due to the subsidiary PFGs, according to their relative abundance. Here, the LCBD was processed for each site and showed it is particularly suitable for high frequency biological monitoring. Indeed, the LCBD confirmed the spatiotemporal heterogeneity observed on the abundance. The biggest and significant changes in community composition are more likely to be observed in coastal areas under freshwater influence.

In the EEC and SNS, the distance to the shore (Baretta-Bekker et al., 2009) and the salinity (Desmit et al., 2015) are important structuring features for plankton. Both are correlated with nutrients because high nutrient concentrations are brought by a variety of freshwater inputs due to river as well as land disperse runoff (Ruddick and Lacroix, 2006) compared to low but constant inputs of the Atlantic Ocean, especially in English Channel and southern North Sea offshore waters through the Strait of Dover. The bottleneck effect of the Dover Strait contributed to drive Atlantic waters to the southern North Sea through the English Channel. These hydrological effects combined to the number of estuaries result in a well–marked separation between brackish water formed by rivers run-offs and offshore mid–Channel Atlantic waters, both flowing northwards. Brackish-salty waters boundary is marked by a tidal front in which brackish waters from the "Coastal flow" in the EEC (Brylinski and Lagadeuc, 1990) and the "Coastal river" in the SNS (Baretta-Bekker et al., 2009). The fact that NanoFLR and microphytoplankton groups contributed less to the total abundance as the distance to the coast increased in areas under freshwater influence was consistent with the theory of enrichment (Riebesell, 1974). On the contrary, the distribution of Coccolithophores abundance increased with the distance to the coast in the SNS, forming high abundance patches in central North Sea waters close to the Dogger Bank, as previously described by Charalampopoulou et al. (2011).

4.2.2 LCBD–water types model

Our study is the first to link the LCBD with environmental and spatial parameters for marine phytoplankton. Although the local environmental and spatial variables significantly explained sites contribution to β-diversity, the explaining variables of our model did not strongly explain the LCBD (R^2 adj.LCBD = 37 %). Our model result is comparable with only few studies which have explored such relationships on invertebrates (Heino and Grönroos, 2017) or zooplankton (da Silva Brito et al., 2020). The comparison between the R^2 adj.LCBD of the previous studies (Heino and Grönroos, 2017; da Silva Brito et al., 2020) and ours suggests a variable relation between the β-diversity index and environmental factors. Such variable relation may be explained by the relevance of the set of environmental variables used to model the LCBD. Indeed, in Heino and Grönroos (2017) and da Silva Brito et al. (2020), the variables used in the model were known as structuring for the invertebrates and zooplankton, while in our study salinity and the distance to the coast are not known to be main structuring variables for marine phytoplankton whereas temperature is known to regulate only some species, such as *P. globosa* in our case (Verity et al., 1988). However, as the scope of our study concern only coastal phytoplankton communities, salinity and temperature were expected to be structuring variables for the abundance of our PFGs. The high LCBD values were indeed observed under low salinity and high temperature revealing the inshore-offshore dilution of the freshwater inputs.

Despite the high correlation of salinity and nutrients (Desmit et al., 2015), adding nutrient data collected at high spatial resolution would have increased the relevance of the model. Monitoring the nutrient at high resolution should be applied in our study area representing a major improvement in studying small scales processes affecting phytoplankton (Hydes et al., 2010; Pellerin et al., 2016; Vuillemin et al., 2009). In this way, recent development of the Water In situ analyZer (WIZ, Systea, Italy) in collaboration with IFREMER are promising.

4.3 PFGs characteristics

4.3.1 Niche distribution and overlap

As stated by several authors (Cullen et al., 1997; Glibert, 2016; Margalef, 1978; Reynolds, 2006), spatiotemporal heterogeneity of the Phytoplankton Functional Types (PFT) defined from species abundance highlights the concept of life-form adaptation to pelagic habitats (i.e. spatial niche). In flow cytometry studies, it is more adequate to define the groups as Phytoplankton Functional Groups (PFGs) according to Reynolds (1997) definition for two reasons: first, the PFG definition is more general compared to the PFT definition because flow cytometry is not able to characterize the biogeochemical features of the groups and because the definition of groups is not based on taxonomy (it is based on optical properties of cells and colonies related to morphology, size and pigment composition). Secondly, it has already been shown that the traits at the level of the PFG used in flow cytometry are to some extent reliable to detect different ecological strategies (Breton et al., 2017; Fragoso et al., 2019; Fontana et al., 2018; Litchman et al., 2007; Litchman and Klausmeier, 2008; Pomati and Nizzetto, 2013).

Our study showed differences in the niche position and niche tolerance between the phytoplankton groups having consequences on the niche overlap between PFGs. These differences were due to the environmental parameters, e.g. temperature, salinity, distance to shore and bathymetry, showing a trade-off in the space used and in time. Consequently, the spatiotemporal distribution of the PFGs resulted in a trade-off in the use of the resources (Breton et al., 2017). However, all the PFGs defined in the present study showed a high residual tolerance, arguing that a high proportion of the spatiotemporal variability is not only explained by our limited environmental set of variables. Indeed, as mentioned in the previous part, other factors should have been considered such as physico-chemical (e.g. nutrients), physical (e.g. turbulence, currents, wind stress) or physiological/biological factors (e.g. photosynthetic parameters, competition, parasitism, predation, viral lysis). For example, other temperate coastal studies focusing on low frequency discrete long-term sampling series (Hernández-Fariñas et al., 2015; Heino and Soininen, 2006; Karasiewicz et al., 2018) addressed phytoplankton species connection with nutrients, which are known to be important parameters of phytoplankton temporal distribution. In those studies, residual tolerances were variable and sometimes particularly high (15 % to 94 % in Heino and Soininen, 2006; 55 % to 87 % in Hernández-Fariñas et al. (2015); 46 % to 84 % in Karasiewicz et al. (2018)). The residual tolerances calculated in our study were in the same range (28 % to 86 %). Consequently, adding only nutrients might not have provided better explanation of the niche parameters. Moreover, the results of the permutation tests were significant and demonstrate that the variables used in our study significantly explained the distribution of the PFGs during the month considered in the area considered. Although some structuring variables were missing in HF analyses, the main aim of our study was to investigate the high spatiotemporal resolution of the PFGs configuration during the spring bloom development, according to abiotic and spatial features influencing their distribution. Some physico-chemical variables measured on discrete stations were then considered for niche repartition and overlap over 1-dimension.

In the present study, the environmental and spatial variables explained between 12.4 % and 55.2 % of the inertia of the PFGs. As we characterized spatiotemporal niches of our PFGs, a marginal PFG is spatially restricted to small areas. They usually form well-located tiny patches. Such PFGs can be restraint due to interactions with other PFGs, by being low competitors, by selective predation or parasitism, but also, they can be restraint by the resources, which can be non-optimal for their develop-

ment. In the opposite, a non-marginal PFG is common of the study area during the sample period. Such observations occur when they form large bloom of biomass and abundance. Here, Cryptophytes and two life stages of *P. globosa* (NanoHighFLR and NanoVeryHighFLR) exhibited the lowest marginality meaning their spatial niche was wide during the period considered, thus exhibiting a large spatial distribution. On the contrary, PFGs exhibiting high marginality such as PicoHighFLR, Coccolithophores and *Pseudo-nitzschia* occurred in less common habitats in mid spring, which means, here, that their spatial distribution is confined to some specific areas, defining their spatial distribution as highly patchy. In addition, widespread PFGs were also observed to be more tolerant to environment changes than the spatially restricted PFGs which were more constraint by the environment defined in this study. Moreover, as the *P. globosa* bloom are usually dominated by up to 80 % of this species (Breton et al., 2000; Lefebvre et al., 2011; Schapira et al., 2008), the last 20 % remained for the other groups which made them more constraint by the environmental conditions. Indeed, considering the "silicate-*Phaeocystis* hypothesis" (Lancelot et al., 1987; Reid et al., 1990) and the phosphorus depletion hypothesis (Egge, 1998) in diatoms growth, the silicate and phosphorus depletions after or during the decaying phase of the diatom bloom (not sampled during our cruises) allowed *P. globosa* to bloom and reduce the habitat of diatoms (Litchman and Klausmeier, 2008), hence reducing the silicate and phosphorus niches for diatoms (forming part of the microphytoplankton group) including the *Pseudo-nitzschia* group. However, *Pseudo-nitzschia* may be favorished against the microphytoplankton group (diatoms and pigmented dinoflagellates) by two mechanisms: it is highly competitive for nutrients and it is also epiphyte of *P. globosa* which was supported with a detection of *Pseudo-nitzschia* spp. in water types with various N:P ratios, i.e. in both low (N:P < 16) and high N:P (N:P > 16; Fig. 8). On the other hand, *P. globosa* single cell morphotypes were associated with water types characterized by a ratio of N:P higher than 16. These results confirm that *Pseudo-nitzschia* spp. and *P. globosa* development are stimulated by nitrogen inputs (Cadée and Hegeman, 1991; Carter et al., 2005; Claquin et al., 2010; Downes-Tettmar et al., 2013; Liefer et al., 2009; Parsons et al., 2013; Riegman et al., 1990; Thorel et al., 2017), whereas the rest of the microphytoplankton (called here "Microphytoplankton", mainly composed by diatoms and few pigmented dinoflagellates (Louchart et al., 2018)) are observed in water types with low N:P because microphytoplankton growth requires high concentration of silicates and/or phosphorus (Thorel et al., 2017). Here, the microphytoplankton PFG which is quasi-exclusively represented by diatoms and pigmented dinoflagellates, showed affinity for high Si:P and low Si:N. These results clearly explained an imbalance between the nutrients. The low Si:N states a silicate depletion and a high Si:P results of a strong depletion of phosphorus. Consequently, the dominance of *P. globosa* over microphytoplankton, in terms of abundance, would refer to silicate depletion and/or phosphate depletion hypotheses as *P. globosa* is known to be able to cope on P depletion (van Boekel, 1992; Riegman et al., 1992). On the contrary, cryptophytes, which are ubiquitous with a wide niche breadth, are known to be a stress-tolerant group (Margalef, 1978) occurring after disturbance. Such in situ observations were also congruent with temporal monitoring, pointing out their presence in April-May in this area (Bonato et al., 2015; Schapira et al., 2008). The abundance of coccolithophores is reported to be low along the coast of the EEC and SNS, with a fast increase of five orders of magnitude in few kilometers in Central North Sea waters getting closer to the Dogger Bank. This area regularly suffers of the lack of study of the marginal groups of phytoplankton. Only a few observations were previously reported, mainly in summer (Charalampopoulou et al., 2011; Holligan et al., 1993). Holligan et al. (1993) observed that the coccolithophore *Emiliania huxleyi* bloomed just after the diatoms when inorganic nutrients were depleted.

Consequently, after the diatom bloom, *P. globosa* dominates rich nutrient water types along the coast and restraint the low environmental-tolerant (i.e. small niche breadth) coccolithophores to offshore waters of the southern North Sea.

Picoeukaryotes (i.e. *Synechococcus*, PicoVeryLowFLR, PicoLowFLR and PicoHighFLR) can be segregated into two parts according to their niche parameters. Picoeukaryote groups (except *Synechococcus*) might be inferred to *Picomonas* spp. and Picobiliphyta, two groups regularly detected by molecular analysis in the eastern English Channel during the spring blooms (Christaki et al., 2014; Genitsaris et al., 2015; Rachik et al., 2018). On one side, PicoHighFLR was very marginal and had a high tolerance to the environment following the same pattern of niche analysis as the coccolithophores (e.g. abundance of both PFG increased together with the distance to the coast). Hence, PicoHighFLR was restricted to offshore waters and the high environmental tolerance mean that it was observed in a large gradient of environmental conditions. In the opposite, *Synechococcus*, PicoVeryLowFLR and PicoLowFLR groups had the same spatiotemporal niche being widespread and having a large tolerance to the set of environmental parameters considered in our analysis. Consequently, they were able to share the same niche (Chen et al., 2011). These three groups exhibited the lowest niche overlap with the three life-stages of *P. globosa*. The coastal ecosystem classification (Cebrián and Valiela, 1999) may explain the spatial segregation. According to Bonato et al. (2015), the French EEC coast can be considered as an Enclosed Coastal Ecosystem (ECE) dominated successively from late winter to late spring by microphytoplankton (mainly diatoms) and by nanophytoplankton especially *P. globosa*. In the opposite, the Atlantic waters flowing towards the northeast in the English Channel are forming the offshore waters of both the English Channel and the southern North Sea. These areas can be considered as Open Coastal Ecosystem (OCE). Such ecosystem is dominated by picophytoplankton. Because the water masses of the English Channel are drifting towards the North Sea, the ECE defines a continuum of brackish waters from the Bay of Seine to the Wadden Islands (Desmit et al., 2015), interrupted by some temporal and spatial discontinuities, as in the Normandy coasts and southern par of the Belgian Coastal Zone which are both OCE.

Low overlap values between Microphytoplankton and *Pseudo-nitzschia* groups versus *P. globosa* life-stages are supported by the phenology of the blooms. Indeed, in spring, the timing and the amplitude of the blooms are strongly dependent of the nutrient stock and the light availability. This result is also supported by the high abundance of the different life-stages of *P. globosa* along the coast (Lancelot et al., 1987). The relatively higher niche overlap between *P. globosa* and *Pseudo-nitzschia* spp. reveals a spatiotemporal co-occurrence of the two groups. Some differences highlighted by the N:P and Si:N ratios showed that niches of single-cell stages of *P. globosa* and *Pseudo-nitzschia* spp. are different. However, the colonial stage of *P. globosa* and *Pseudo-nitzschia* spp. share the same nutrient niche revealing that *P. globosa* and *Pseudo-nitzschia* spp. co-occur in space. This observation is supported by the fact that during the transition between the *P. globosa* single-cell to the colonial stage and when colonies are of a sufficient size, *Pseudo-nitzschia* can use *P. globosa* as habitat (Sazhin et al., 2007).

4.3.2 SCBD–niches parameter model

We have demonstrated that the application of the SCBD to the PFGs is ecologically relevant. Our findings across water types highlight that Species Contribution to β–diversity (SCBD) considering Phytoplankton Functional Groups (PFGs) depends on the abundance of the PFGs as well as their niche characteristics. We found negative and significant relation between the SCBD

and the niche position and positive but weak relation between SCBD and niche breadth. This result agrees with previous studies showing that, at sub-regional scales, niche position is better than niche breadth to address the contribution of the PFGs to the β–diversity (Heino and Grönroos, 2014; Tonkin et al., 2016). Nevertheless, our model performed weaker relation between the niche position and SCBD than other studies (Heino and Grönroos, 2017; da Silva et al., 2018). We speculate that the difference may be related to two reasons which may be explored in a future survey. First, our consideration of niche characteristics are limited by the temporal extend of the measurements. The present survey only targeted the spring productive period (i.e. the bloom) which missed the non productive period corresponding mainly to June to early-March. Extreme values of temperature and salinity occurring in winter and summer periods must have considerably changed the niche size. Furthermore, niche characteristics are also limited by the number of structural environmental parameters. In the eastern English Channel and southern North Sea, nutrients, current, fronts are non-exhaustive parameters important in phytoplankton community structure and distribution affecting niches size (Karasiewicz et al., 2018). The second reason of the weak relationship suggest stronger relation between PFGs and their SCBD by connecting additional intrinsic parameters of the PFGs to the model. Indeed, despite traits importance remained discussed (da Silva et al., 2018) or minored in comparison to niche characteristics (Heino and Grönroos, 2017, 2014), they have been related to SCBD (Heino and Grönroos, 2017). However, traits strongly support phytoplankton communities structure (Litchman et al., 2007). Consequently, as the optical properties derived from the PFGs can be assimilated to optical traits (Fragoso et al., 2019), we assume the CytoSense may represent a unique opportunity for future investigation of the relation between PFGs characteristics (traits-niche) and the SCBD using in situ data.

Understanding the key determinants to LCBD and SCBD is important for community ecology as well as biomanagement. However, only LCBD has been explored in the past for the purpose of plankton management (Rombouts et al., 2019). As niche is found as a good predictor of the SCBD of the PFGs, we are now able to relate more precisely how the PFGs can evolve in changing environmental conditions at local scales and over short-term periods. From a management perspective, the relationship between niche and SCBD will therefore help understanding which environmental condition is better to target to impact the development of some taxa or phytoplankton group. This is particularly crucial in the management of harmful algae to reduce the amplitude and the timing of their blooms. At larger scales (regional or broad scale), the application of this methodology to long-term plankton monitoring may provide better explanation how pressures such as eutrophication and climate change can act within each species of the plankton communities. We may therefore be able to predict their development in the context of broad scale environmental changes.

5 Conclusions

In this study we found high spatio-temporal variability of phytoplankton community during the spring bloom in the eastern English Channel and southern North Sea. This patchiness in phytoplankton distribution resulted in dynamic environmental conditions. As consequence, the patchiness highlighted segregation of the phytoplankton functional groups (PFGs) which was successfully highlighted by connecting the concept of the niche to phytoplankton groups discriminated by flow cytometry. While cruising over the eastern English Channel and southern North Sea, changes in community composition and the con-

tribution of each PFG occurred. Both were modelled by β–diversity indices (LCBD and SCBD) which could be predicted by environmental conditions and intrinsic parameter of each PFG. Based on our original research, future investigations should therefore include modelling β–diversity indices to report and then predict plankton communities evolution and the contribution of each plankton unit by linking ecological features (niche and traits) and pressures at both short (e.g. extrem event such as strong, precipitations) and long term (e.g. climate change).

In Europe, management of marine waters is supported by the member states of the OSPAR commission through the MSFD. This directive connects the ICG–COBAM (OSPAR) Pelagic Habitat Indicators (PH1/FW5 "changes in plankton lifeforms", PH2 "changes in plankton biomass/abundance" and PH3 "changes in plankton diversity") to both abiotic and biotic parameters to better understand the environmental status of marine ecosystems. As β–diversity indices part of the methodology of the ICG-COBAM PH3, we strongly support the fact that the flow cytometer mounted onboard research vessels and/or ships-of-opportunity could be a powerful tool for investigating the pelagic habitats where traditional fixed station monitoring could not assessed marine waters and where continuous monitoring are more suitable for zooplankton rather than phytoplankton collection. In this purpose, current collaborative initiatives within European projects (i.e. H2020 INFRAIA JERICO–S3) as well as developing regular monitoring of offshore waters will add offshore view of the ICG–COBAM Pelagic Habitat indicators across the large–spatial areas.

Appendix A

Table A1. Mean $\pm$ sd of the environmental variables (temperature, salinity, distance to the shore and bathymetry) among the eight regions.

Water type	Temperature (degree)	Salinity	Distance to the shore (km)	Bathymetry (m)
1	10.96 ± 0.34	34.33 ± 0.37	18 ± 10	-30 ± 6
2	11.24 ± 0.32	34.39 ± 0.27	7 ± 6	-15 ± 5
3	10.92 ± 0.23	34.42 ± 0.36	19 ± 11	-53 ± 9
4	11.65 ± 0.27	33.09 ± 0.47	9 ± 6	-17 ± 7
5	11.47 ± 0.53	34.92 ± 0.33	62 ± 13	-31 ± 5
6	12.82 ± 0.44	33.41 ± 0.66	21 ± 13	-21 ± 6
7	10.24 ± 0.27	34.49 ± 0.05	110 ± 16	-43 ± 4
8	14.31 ± 0.57	31.45 ± 0.68	8 ± 6	-13 ± 6

Table A2. Mean ± sd of the size of the eleven phytoplankton functional types during PHYCO, VLIZ and RWS cruise.

Phytoplankton functional type	Mean ± sd (µm)
Synechococcus	1.99 ± 0.45
PicoVeryLowFLR	2.48 ± 0.65
PicoLowFLR	2.18 ± 0.37
PicoHighFLR	2.31 ± 0.42
Cryptophytes	5.27 ± 2.47
Coccolithophores	7.06 ± 2.31
NanoLowFLR	4.71 ± 0.38
NanoHighFLR	3.58 ± 0.78
NanoVeryHighFLR	6.11 ± 2.31
Pseudo-nitzschia	18.87 ± 4.78
Microphytoplankton	33.45 ± 10.25

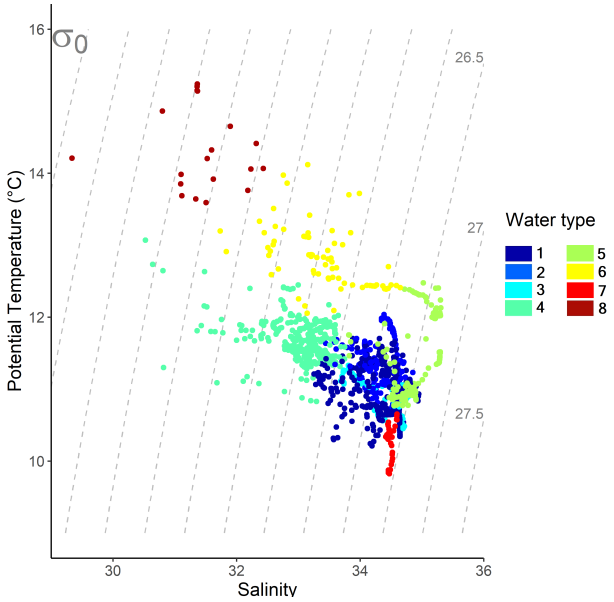

Figure A1. Temperature-salinity diagram and the eight water types.

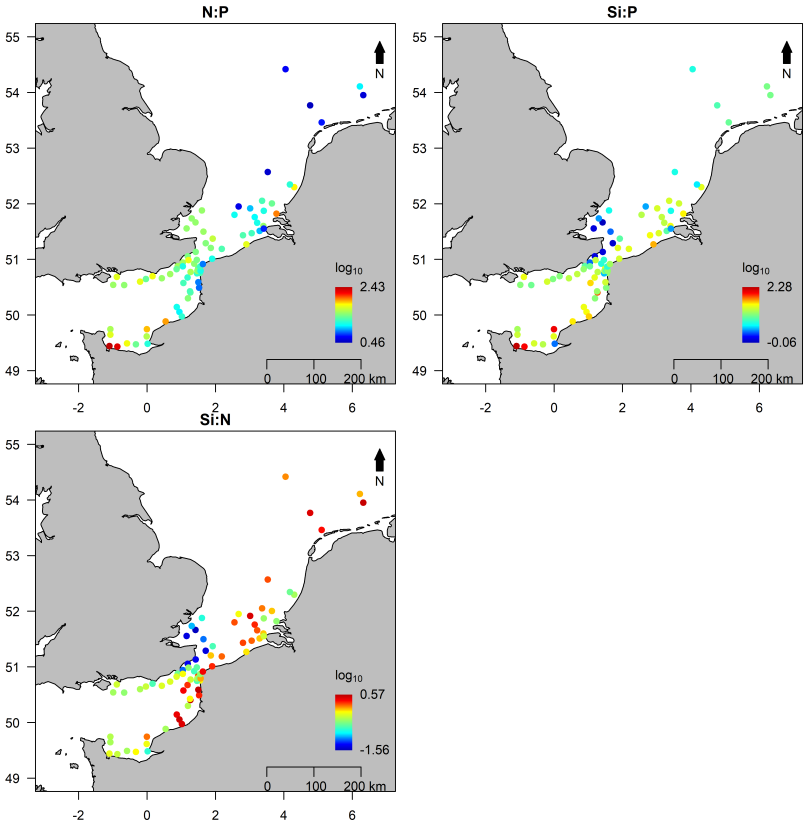

Figure A2. Log10 of the nutrients ratios.

Author contributions. AL participated to cruises and processed the flow cytometry data on the RVs *Côtes de la Manche*, *Simon Stevin* and *Zirfaea*. LFA, JM and MR conceived the study, were respectively in charge of the analysis onboard the RVs *Côtes de la Manche* (CNRS INSU, PHYCO cruise), *Simon Stevin* (VLIZ, Lifewatch-JERICO cruise) and *Zirfaea* (RWS, MWTL Cruise). EL and MC processed nutrients analysis. AL carried out statistical analyses and led the manuscript and participated to the writing with LFA, FGS and FL. LFA, AL, FL, JM, KD, MR and ED participated to discussions for the elaboration of this paper. All authors commented all phase of writing and contributed to proofread the manuscript.

Competing interests. The authors declare that they have no conflict of interest.

Acknowledgements. AL was co-funded by a PhD grant from the "Université du Littoral-Côte d'Opale" and an "Hauts-de-France" Regional research fellowship. He was also funded by a research fellowship grant of PON PLaCE ARS01_00891 of the Stazione Zoologica Anton Dohrn and is currently funded by an IFREMER LER/BL contract. This work has been financially supported by the European Union (ERDF), the French State, the French Region Hauts-de-France and Ifremer, in the framework of the project CPER MARCO 2015-2021. PHYCO–cruise was funded by the JERICO–NEXT project and the MTES/ CNRS convention for the MSFD and Monitoring Programme implementation in Pelagic Habitats of France. Funding for the VLIZ cruise, e.g. data collection and infrastructure (RV *Simon Stevin*), were provided by VLIZ as part of the Flemish contribution to LifeWatch ESFRI. The Vliz cruise as well as the RWS cruise were funded by the JERICO–NEXT project. The JERICO–NEXT project has received funding from the European Union's Horizon 2020 research and innovation programme under grant agreement no. 654410. We thank the crew and the Captain of the research vessels *Côtes de la Manche* (CNRS INSU), *Simon Stevin* (VLIZ) and *Zirfaea* (RWS), as well as the scientific and technical staff of the different institutes involved (LOG, VLIZ and RWS). We also thank the heads of mission of the Belgian (Lennert Tyberghein, VLIZ) and Dutch (Arnold Veen, RWS) cruises. We are thanfull to Dr. Fernando Gómez (University of Salento) for carrying the microscopy counts of the PHYCO cruise and his remarks on this manuscript. We are thankfull to Eric Lécuyer for the ammonia analysis of the PHYCO cruise.

References

Aardema, H. M., Rijkeboer, M., Lefebvre, A., Veen, A., and Kromkamp, J. C.: High-resolution underway measurements of phytoplankton photosynthesis and abundance as an innovative addition to water quality monitoring programs, Ocean Sci., 15, 1267–1285, 2019.

Aminot, A. and Kérouel, R.: Hydrologie des écosystèmes marins: paramètres et analyses, Editions Quae, 2004.

Baretta-Bekker, J., Baretta, J., Latuhihin, M., Desmit, X., and Prins, T.: Description of the long-term (1991–2005) temporal and spatial distribution of phytoplankton carbon biomass in the Dutch North Sea, J. Sea Res., 61, 50–59, 2009.

Bonato, S., Christaki, U., Lefebvre, A., Lizon, F., Thyssen, M., and Artigas, L. F.: High spatial variability of phytoplankton assessed by flow cytometry, in a dynamic productive coastal area, in spring: The eastern English Channel, Estuar. Coast. Shelf S., 154, 214–223, 2015.

Bonato, S., Breton, E., Didry, M., Lizon, F., Cornille, V., Lécuyer, E., Christaki, U., and Artigas, L. F.: Spatio-temporal patterns in phytoplankton assemblages in inshore–offshore gradients using flow cytometry: A case study in the eastern English Channel, J. Mar. Syst., 156, 76–85, 2016.

Breton, E., Brunet, C., Sautour, B., and Brylinski, J.-M.: Annual variations of phytoplankton biomass in the Eastern English Channel: comparison by pigment signatures and microscopic counts, J. Plankton Res., 22, 1423–1440, 2000.

Breton, E., Rousseau, V., Parent, J.-Y., Ozer, J., and Lancelot, C.: Hydroclimatic modulation of diatom/Phaeocystis blooms in nutrient-enriched Belgian coastal waters (North Sea), Limnol. Oceanogr., 51, 1401–1409, 2006.

Breton, E., Christaki, U., Bonato, S., Didry, M., and Artigas, L. F.: Functional trait variation and nitrogen use efficiency in temperate coastal phytoplankton, Mar. Ecol. Prog. Ser., 563, 35–49, 2017.

Broennimann, O., Fitzpatrick, M. C., Pearman, P. B., Petitpierre, B., Pellissier, L., Yoccoz, N. G., Thuiller, W., Fortin, M.-J., Randin, C., Zimmermann, N. E., et al.: Measuring ecological niche overlap from occurrence and spatial environmental data, Global Ecol. Biogeogr., 21, 481–497, 2012.

Brunet, C. and Lizon, F.: Tidal and diel periodicities of size-fractionated phytoplankton pigment signatures at an offshore station in the southeastern English Channel, Estuar. Coast. Shelf S., 56, 833–843, 2003.

Brussaard, C., Gast, G., Van Duyl, F., and Riegman, R.: Impact of phytoplankton bloom magnitude on a pelagic microbial food web, Mar. Ecol. Prog. Ser., 144, 211–221, 1996.

Brylinski, J., Lagadeuc, Y., Gentilhomme, V., Dupont, J., Lafite, R., Dupeuble, P., Huault, M., and Auger, Y.: Le fleuve côtier: un phénomène hydrologique important en Manche Orientale. Exemple du Pas-de-Calais, Oceanol. Acta, 1991.

Brylinski, J., Brunet, C., Bentley, D., Thoumelin, G., and Hilde, D.: Hydrography and phytoplankton biomass in the eastern English Channel in spring 1992, Estuar. Coast. Shelf S., 43, 507–519, 1996.

Brylinski, J.-M. and Lagadeuc, Y.: L'interface eaux côtières/eaux du large dans le Pas-de-Calais (côte française): une zone frontale, C.R. Acad. Sci. II, 311, 535–540, 1990.

Cadée, G. C. and Hegeman, J.: Historical phytoplankton data of the Marsdiep, Hydrobiol. Bull., 24, 111–118, 1991.

Carter, C., Ross, A., Schiel, D., Howard-Williams, C., and Hayden, B.: In situ microcosm experiments on the influence of nitrate and light on phytoplankton community composition, J. Exp. Mar. Biol. and Ecol., 326, 1–13, 2005.

Cebrián, J. and Valiela, I.: Seasonal patterns in phytoplankton biomass in coastal ecosystems, J. Plankton Res., 21, 429–444, 1999.

Charalampopoulou, A., Poulton, A. J., Tyrrell, T., and Lucas, M. I.: Irradiance and pH affect coccolithophore community composition on a transect between the North Sea and the Arctic Ocean, Mar. Ecol. Prog. Ser., 431, 25–43, 2011.

Chen, B., Wang, L., Song, S., Huang, B., Sun, J., and Liu, H.: Comparisons of picophytoplankton abundance, size, and fluorescence between summer and winter in northern South China Sea, Cont. Shelf Res., 31, 1527–1540, 2011.

Christaki, U., Kormas, K. A., Genitsaris, S., Georges, C., Sime-Ngando, T., Viscogliosi, E., and Monchy, S.: Winter–summer succession of unicellular eukaryotes in a meso-eutrophic coastal system, Microb. Ecol., 67, 13–23, 2014.

Claquin, P., Longphuirt, S. N., Fouillaron, P., Huonnic, P., Ragueneau, O., Klein, C., and Leynaert, A.: Effects of simulated benthic fluxes on phytoplankton dynamic and photosynthetic parameters in a mesocosm experiment (Bay of Brest, France), Estuar. Coast. Shelf S., 86, 93–101, 2010.

Costanza, R., d'Arge, R., De Groot, R., Farber, S., Grasso, M., Hannon, B., Limburg, K., Naeem, S., O'neill, R. V., Paruelo, J., et al.: The value of the world's ecosystem services and natural capital, Ecol. Econ., 25, 3–15, 1998.

Cullen, J. J., Ciotti, A. M., Davis, R. F., and Lewis, M. R.: Optical detection and assessment of algal blooms, Limnol. Oceanogr., 42, 1223–1239, 1997.

Cullen, J. J., Franks, P. J., Karl, D. M., and Longhurst, A.: Physical influences on marine ecosystem dynamics, The sea, 12, 297–336, 2002.

da Silva, P. G., Hernández, M. I. M., and Heino, J.: Disentangling the correlates of species and site contributions to beta diversity in dung beetle assemblages, Divers. Distrib., 24, 1674–1686, 2018.

da Silva Brito, M. T., Heino, J., Pozzobom, U. M., and Landeiro, V. L.: Ecological uniqueness and species richness of zooplankton in subtropical floodplain lakes, Aquat. Sci., 82, 1–13, 2020.

Derot, J., Schmitt, F. G., Gentilhomme, V., and Zongo, S. B.: Long-term high frequency phytoplankton dynamics, recorded from a coastal water autonomous measurement system in the eastern English Channel, Cont. Shelf Res., 109, 210–221, 2015.

Desmit, X., Ruddick, K., and Lacroix, G.: Salinity predicts the distribution of chlorophyll a spring peak in the southern North Sea continental waters, J. Sea Res., 103, 59–74, 2015.

Dolédec, S., Chessel, D., and Gimaret-Carpentier, C.: Niche separation in community analysis: a new method, Ecology, 81, 2914–2927, 2000.

Downes-Tettmar, N., Rowland, S., Widdicombe, C., Woodward, M., and Llewellyn, C.: Seasonal variation in Pseudo-nitzschia spp. and domoic acid in the Western English Channel, Cont. Shelf Res., 53, 40–49, 2013.

Dubelaar, G. B., Gerritzen, P. L., Beeker, A. E., Jonker, R. R., and Tangen, K.: Design and first results of CytoBuoy: A wireless flow cytometer for in situ analysis of marine and fresh waters, Cytometry, 37, 247–254, 1999.

Dugenne, M., Thyssen, M., Nerini, D., Mante, C., Poggiale, J.-C., Garcia, N., Garcia, F., and Grégori, G. J.: Consequence of a sudden wind event on the dynamics of a coastal phytoplankton community: an insight into specific population growth rates using a single cell high frequency approach, Front. Microbiol., 5, 485, 2014.

Egge, J.: Are diatoms poor competitors at low phosphate concentrations?, J. Mar. Syst., 16, 191–198, 1998.

Fontana, S., Jokela, J., and Pomati, F.: Opportunities and challenges in deriving phytoplankton diversity measures from individual trait-based data obtained by scanning flow-cytometry, Front. Microbiol., 5, 324, 2014.

Fontana, S., Thomas, M. K., Moldoveanu, M., Spaak, P., and Pomati, F.: Individual-level trait diversity predicts phytoplankton community properties better than species richness or evenness, ISME J., 12, 356–366, 2018.

Fragoso, G. M., Poulton, A. J., Pratt, N. J., Johnsen, G., and Purdie, D. A.: Trait-based analysis of subpolar North Atlantic phytoplankton and plastidic ciliate communities using automated flow cytometer, Limnol. Oceanogr., 64, 1763–1778, 2019.

Gaston, K. and Blackburn, T.: Pattern and process in macroecology, John Wiley & Sons, 2008.

Gaston, K. J., Blackburn, T. M., and Lawton, J. H.: Interspecific abundance-range size relationships: an appraisal of mechanisms, J. Anim. Ecol., pp. 579–601, 1997.

Genitsaris, S., Monchy, S., Viscogliosi, E., Sime-Ngando, T., Ferreira, S., and Christaki, U.: Seasonal variations of marine protist community structure based on taxon-specific traits using the eastern English Channel as a model coastal system, FEMS Microbiol. Ecol., 91, fiv034, 2015.

Genitsaris, S., Monchy, S., Breton, E., Lecuyer, E., and Christaki, U.: Small-scale variability of protistan planktonic communities relative to environmental pressures and biotic interactions at two adjacent coastal stations, Mar. Ecol. Prog. Ser., 548, 61–75, 2016.

Glibert, P. M.: Margalef revisited: a new phytoplankton mandala incorporating twelve dimensions, including nutritional physiology, Harmful Algae, 55, 25–30, 2016.

Gómez, F. and Souissi, S.: Unusual diatoms linked to climatic events in the northeastern English Channel, J. Sea Res., 58, 283–290, 2007.

Grattepanche, J.-D., Breton, E., Brylinski, J.-M., Lecuyer, E., and Christaki, U.: Succession of primary producers and micrograzers in a coastal ecosystem dominated by Phaeocystis globosa blooms, J. Plankton Res., 33, 37–50, 2011.

Guiselin, N.: Etude de la dynamique des communautés phytoplanctoniques par microscopie et cytométrie en flux, en eaux côtières de la Manche orientale, ULCO-MREN, Doctorate (Ph. D.) Thesis in Biological Oceanology, University of Littoral Côte d'Opale (ULCO), 2010.

Heino, J.: Positive relationship between regional distribution and local abundance in stream insects: a consequence of niche breadth or niche position?, Ecography, 28, 345–354, 2005.

Heino, J. and Grönroos, M.: Untangling the relationships among regional occupancy, species traits, and niche characteristics in stream invertebrates, Ecol. Evol., 4, 1931–1942, 2014.

Heino, J. and Grönroos, M.: Exploring species and site contributions to beta diversity in stream insect assemblages, Oecologia, 183, 151–160, 2017.

Heino, J. and Soininen, J.: Regional occupancy in unicellular eukaryotes: a reflection of niche breadth, habitat availability or size-related dispersal capacity?, Freshwater Biol., 51, 672–685, 2006.

Hernández-Fariñas, T., Bacher, C., Soudant, D., Belin, C., and Barillé, L.: Assessing phytoplankton realized niches using a French national phytoplankton monitoring network, Estuar. Coast. Shelf S., 159, 15–27, 2015.

Holligan, P. M., Groom, S. B., and Harbour, D. S.: What controls the distribution of the coccolithophore, Emiliania huxleyi, in the North Sea?, Fish. Oceanogr., 2, 175–183, 1993.

Houliez, E., Lizon, F., Thyssen, M., Artigas, L. F., and Schmitt, F. G.: Spectral fluorometric characterization of Haptophyte dynamics using the FluoroProbe: an application in the eastern English Channel for monitoring Phaeocystis globosa, J. Plankton Res., 34, 136–151, 2012.

Hutchinson, G. E.: Concluding remarks, Cold Spring Harb. Sym., 22, 415–427, 1957.

Hydes, D., Aoyama, M., Aminot, A., Bakker, K., Becker, S., Coverly, S., Daniel, A., Dickson, A., Grosso, O., Kerouel, R., Ooijen, J., Sato, K., Tanhua, T., Woodward, E., and Zhang, J.-Z.: Determination of dissolved nutrients (N, P, Si) in seawater with high precision and inter-comparability using gas-segmented continuous flow analysers, in: The GO-SHIP Repeat Hydrography Manual : A Collection of Expert Reports and guidelines. IOCCP Report No 14, ICPO Publication Series No. 134, version 1, 2010, Paris: UNESCO/ICO, 2010.

Karasiewicz, S., Dolédec, S., and Lefebvre, S.: Within outlying mean indexes: refining the OMI analysis for the realized niche decomposition, PeerJ, 5, e3364, 2017.

Karasiewicz, S., Breton, E., Lefebvre, A., Fariñas, T. H., and Lefebvre, S.: Realized niche analysis of phytoplankton communities involving HAB: Phaeocystis spp. as a case study, Harmful Algae, 72, 1–13, 2018.

Lacroix, G., Ruddick, K., Ozer, J., and Lancelot, C.: Modelling the impact of the Scheldt and Rhine/Meuse plumes on the salinity distribution in Belgian waters (southern North Sea), J. Sea Res., 52, 149–163, 2004.

Lamy, D., Obernosterer, I., Laghdass, M., Artigas, L., Breton, E., Grattepanche, J., Lecuyer, E., Degros, N., Lebaron, P., and Christaki, U.: Temporal changes of major bacterial groups and bacterial heterotrophic activity during a Phaeocystis globosa bloom in the eastern English Channel, Aquat. Micro Ecol., 58, 95–107, 2009.

Lancelot, C., Billen, G., Sournia, A., Weisse, T., Colijn, F., Veldhuis, M. J., Davies, A., and Wassmann, P.: Phaeocystis blooms and nutrient enrichment in the continental coastal zones of the North Sea, Ambio, 1987.

Lefebvre, A., Guiselin, N., Barbet, F., and Artigas, F. L.: Long-term hydrological and phytoplankton monitoring (1992–2007) of three potentially eutrophic systems in the eastern English Channel and the Southern Bight of the North Sea, ICES J. Mar. Sci., 68, 2029–2043, 2011.

Legendre, P. and De Cáceres, M.: Beta diversity as the variance of community data: dissimilarity coefficients and partitioning, Ecol. Lett., 16, 951–963, 2013.

Liefer, J. D., MacIntyre, H. L., Novoveská, L., Smith, W. L., and Dorsey, C. P.: Temporal and spatial variability in Pseudo-nitzschia spp. in Alabama coastal waters: a "hot spot" linked to submarine groundwater discharge?, Harmful Algae, 8, 706–714, 2009.

Litchman, E. and Klausmeier, C. A.: Trait-based community ecology of phytoplankton, Annu. Rev. Ecol. Evol. S., 39, 615–639, 2008.

Litchman, E., Klausmeier, C. A., Schofield, O. M., and Falkowski, P. G.: The role of functional traits and trade-offs in structuring phytoplankton communities: scaling from cellular to ecosystem level, Ecol. Lett., 10, 1170–1181, 2007.

Louchart, A., de Blok, R., Debuschere, E., Gómez, F., Lefebvre, A., Lizon, F., Mortelmans, J., Rijkeboer, M., Deneudt, K., Veen, A., et al.: Automated techniques to follow the spatial distribution of Phaeocystis globosa and diatom spring blooms in the English Channel and North Sea, HARMFUL ALGAE 2018–FROM ECOSYSTEMS TO SOCIO-ECOSYSTEMS, pp. 51–55, 2018.

Louchart, A., Lizon, F., Lefebvre, A., Didry, M., Schmitt, F. G., and Artigas, L. F.: Phytoplankton distribution from Western to Central English Channel, revealed by automated flow cytometry during the summer-fall transition, Cont. Shelf Res., 195, 104 056, 2020.

Lovejoy, S., Currie, W., Tessier, Y., Claereboudt, M., Bourget, E., Roff, J., and Schertzer, D.: Universal multifractals and ocean patchiness: phytoplankton, physical fields and coastal heterogeneity, J. Plankton Res., 23, 117–141, 2001.

Margalef, R.: Life-forms of phytoplankton as survival alternatives in an unstable environment, Oceanol. Acta, 1, 493–509, 1978.

Monchy, S., Grattepanche, J.-D., Breton, E., Meloni, D., Sanciu, G., Chabé, M., Delhaes, L., Viscogliosi, E., Sime-Ngando, T., and Christaki, U.: Microplanktonic community structure in a coastal system relative to a Phaeocystis bloom inferred from morphological and tag pyrosequencing methods, PLoS ONE, 7, e39 924, 2012.

Mortelmans, J., Deneudt, K., Cattrijsse, A., Beauchard, O., Daveloose, I., Vyverman, W., Vanaverbeke, J., Timmermans, K., Peene, J., Roose, P., et al.: Nutrient, pigment, suspended matter and turbidity measurements in the Belgian part of the North Sea, Sci. data, 6, 1–8, 2019.

Muylaert, K., Gonzales, R., Franck, M., Lionard, M., Van der Zee, C., Cattrijsse, A., Sabbe, K., Chou, L., and Vyverman, W.: Spatial variation in phytoplankton dynamics in the Belgian coastal zone of the North Sea studied by microscopy, HPLC-CHEMTAX and underway fluorescence recordings, J. Sea Res., 55, 253–265, 2006.

Parsons, M. L., Dortch, Q., and Doucette, G. J.: An assessment of Pseudo-nitzschia population dynamics and domoic acid production in coastal Louisiana, Harmful Algae, 30, 65–77, 2013.

Pellerin, B. A., Stauffer, B. A., Young, D. A., Sullivan, D. J., Bricker, S. B., Walbridge, M. R., Clyde Jr, G. A., and Shaw, D. M.: Emerging tools for continuous nutrient monitoring networks: Sensors advancing science and water resources protection, J. Am. Water Resour. As., 52, 993–1008, 2016.

Peperzak, L.: Daily irradiance governs growth rate and colony formation of Phaeocystis (Prymnesiophyceae), J. Plankton Res., 15, 809–821, 1993.

Pereira, G., Figueiredo, A., and Ebecken, N.: Using in situ flow cytometry images of ciliates and dinoflagellates for aquatic system monitoring, Braz. J. Biol., 78, 240–247, 2018.

Pomati, F. and Nizzetto, L.: Assessing triclosan-induced ecological and trans-generational effects in natural phytoplankton communities: a trait-based field method, Ecotoxicology, 22, 779–794, 2013.

Prins, T., Desmit, X., and Baretta-Bekker, J.: Phytoplankton composition in Dutch coastal waters responds to changes in riverine nutrient loads, J. Sea Res., 73, 49–62, 2012.

Quisthoudt, C.: Production primaire phytoplanctonique dans le détroit du Pays-de-Calais (France): variations spatiales et annuelles au large du Cap Gris-Nez, C. R. Acad. Ser. III-Vie, 304, 245–250, 1987.

Rachik, S., Christaki, U., Li, L. L., Genitsaris, S., Breton, E., and Monchy, S.: Diversity and potential activity patterns of planktonic eukaryotic microbes in a mesoeutrophic coastal area (eastern English Channel), PloS ONE, 13, e0196 987, 2018.

Reid, P., Lancelot, C., Gieskes, W., Hagmeier, E., and Weichart, G.: Phytoplankton of the North Sea and its dynamics: a review, Neth. J. Sea Res., 26, 295–331, 1990.

Reynolds, C. S.: Vegetation processes in the pelagic: a model for ecosystem theory, vol. 9, Ecology Institute Oldendorf, 1997.

Reynolds, C. S.: The ecology of phytoplankton, Cambridge University Press, 2006.

Riebesell, J. F.: Paradox of enrichment in competitive systems, Ecology, 55, 183–187, 1974.

Riegman, R., Colijn, F., Malschaert, J., Kloosterhuis, H., and Cadee, G.: Assessment of growth rate limiting nutrients in the North Sea by the use of nutrient-uptake kinetics, Neth. J. Sea Res., 26, 53–60, 1990.

Riegman, R., Noordeloos, A. A., and Cadée, G. C.: Phaeocystis blooms and eutrophication of the continental coastal zones of the North Sea, Mar. Biol., 112, 479–484, 1992.

Rombouts, I., Simon, N., Aubert, A., Cariou, T., Feunteun, E., Guérin, L., Hoebeke, M., McQuatters-Gollop, A., Rigaut-Jalabert, F., and Artigas, L.: Changes in marine phytoplankton diversity: Assessment under the Marine Strategy Framework Directive, Ecol. Indic., 102, 265–277, 2019.

Rousseau, V., Chrétiennot-Dinet, M.-J., Jacobsen, A., Verity, P., and Whipple, S.: The life cycle of Phaeocystis: state of knowledge and presumptive role in ecology, Biogeochemistry, 83, 29–47, 2007.

Ruddick, K. and Lacroix, G.: Hydrodynamics and meteorology of the Belgian Coastal Zone, Current Status of Eutrophication in the Belgian Coastal Zone, edited by V Rousseau, Ch Lancelot & D Cox (Presses Universitaires de Bruxelles, Belgium), pp. 1–15, 2006.

Rutten, T. P., Sandee, B., and Hofman, A. R.: Phytoplankton monitoring by high performance flow cytometry: a successful approach?, Cytom. Part A, 64, 16–26, 2005.

Salmaso, N., Naselli-Flores, L., and Padisak, J.: Functional classifications and their application in phytoplankton ecology, Freshwater Biol., 60, 603–619, 2015.

Sazhin, A. F., Artigas, L. F., Nejstgaard, J. C., and Frischer, M. E.: The colonization of two Phaeocystis species (Prymnesiophyceae) by pennate diatoms and other protists: a significant contribution to colony biomass, in: Phaeocystis, major link in the biogeochemical cycling of climate-relevant elements, pp. 137–145, Springer, 2007.

Schapira, M., Vincent, D., Gentilhomme, V., and Seuront, L.: Temporal patterns of phytoplankton assemblages, size spectra and diversity during the wane of a Phaeocystis globosa spring bloom in hydrologically contrasted coastal waters, J. Mar. Biol. Assoc. UK, 88, 649, 2008.

Schlüter, L., Møhlenberg, F., Havskum, H., and Larsen, S.: The use of phytoplankton pigments for identifying and quantifying phytoplankton groups in coastal areas: testing the influence of light and nutrients on pigment/chlorophyll a ratios, Mar. Ecol. Prog. Ser., 192, 49–63, 2000.

Schoemann, V., Becquevort, S., Stefels, J., Rousseau, V., and Lancelot, C.: Phaeocystis blooms in the global ocean and their controlling mechanisms: a review, J. Sea Res., 53, 43–66, 2005.

Schoener, T. W.: Nonsynchronous spatial overlap of lizards in patchy habitats, Ecology, 51, 408–418, 1970.

Seuront, L., Schmitt, F., Lagadeuc, Y., Schertzer, D., and Lovejoy, S.: Universal multifractal analysis as a tool to characterize multiscale intermittent patterns: Example of phytoplankton distribution in turbulent coastal waters., J. Plankton Res., 21, 1999.

Seuront, L., Vincent, D., and Mitchell, J. G.: Biologically induced modification of seawater viscosity in the Eastern English Channel during a Phaeocystis globosa spring bloom, J. Mar. Syst., 61, 118–133, 2006.

Stelfox-Widdicombe, C., Archer, S., Burkill, P., and Stefels, J.: Microzooplankton grazing in Phaeocystis and diatom-dominated waters in the southern North Sea in spring, J. Sea Res., 51, 37–51, 2004.

Thorel, M., Claquin, P., Schapira, M., Le Gendre, R., Riou, P., Goux, D., Le Roy, B., Raimbault, V., Deton-Cabanillas, A.-F., Bazin, P., et al.: Nutrient ratios influence variability in Pseudo-nitzschia species diversity and particulate domoic acid production in the Bay of Seine (France), Harmful Algae, 68, 192–205, 2017.

Thyssen, M., Alvain, S., Lefebvre, A., Dessailly, D., Rijkeboer, M., Guiselin, N., Creach, V., and Artigas, L.-F.: High-resolution analysis of a North Sea phytoplankton community structure based on in situ flow cytometry observations and potential implication for remote sensing, Biogeosciences, 12, 4051–4066, 2015.

Tonkin, J. D., Heino, J., Sundermann, A., Haase, P., and Jähnig, S. C.: Context dependency in biodiversity patterns of central German stream metacommunities, Freshwater Biol., 61, 607–620, 2016.

van Boekel, W. H. M.: Interactions of Phaeocystis sp. with organic compounds and the microbial foodweb, Ph.D. thesis, University Library Groningen][Host], 1992.

Verity, P. G., Villareal, T., and Smayda, T.: Ecological investigations of blooms of colonial Phaeocystis pouchetti—I. Abundance, biochemical composition, and metabolic rates, J. Plankton Res., 10, 219–248, 1988.

Vuillemin, R., Sanfilippo, L., Moscetta, P., Zudaire, L., Carbones, E., Maria, E., Tricoire, C., Oriol, L., Blain, S., Le Bris, N., et al.: Continuous nutrient automated monitoring on the Mediterranean Sea using in situ flow analyser, in: OCEANS 2009, pp. 1–8, IEEE, 2009.